NASA TECHNICAL NOTE

NASA TN D-6431

NASA TN D-6431

VALIDATION OF A GENERAL PURPOSE AIRBORNE SIMULATOR FOR SIMULATION OF LARGE TRANSPORT AIRCRAFT HANDLING QUALITIES

by Kenneth J. Szalai

Flight Research Center
Edwards, Calif. 93523

NATIONAL AERONAUTICS AND SPACE ADMINISTRATION • WASHINGTON, D. C. • OCTOBER 1971

1. Report No.	2. Government Accession No.	3. Recipient's Catalog No.
NASA TN D-6431		

4. Title and Subtitle	5. Report Date
VALIDATION OF A GENERAL PURPOSE AIRBORNE SIMULATOR FOR SIMULATION OF LARGE TRANSPORT AIRCRAFT HANDLING QUALITIES	October 1971
	6. Performing Organization Code
7. Author(s)	8. Performing Organization Report No.
Kenneth J. Szalai	H-591
9. Performing Organization Name and Address	10. Work Unit No.
NASA Flight Research Center P.O. Box 273 Edwards, California 93523	720-06-00-01-24
	11. Contract or Grant No.
12. Sponsoring Agency Name and Address	13. Type of Report and Period Covered
National Aeronautics and Space Administration Washington, D. C. 20546	Technical Note
	14. Sponsoring Agency Code

15. Supplementary Notes

16. Abstract

A flight simulation program was conducted to validate the general purpose airborne simulator (GPAS) for handling-qualities studies of large transport aircraft in cruise. Pilots compared flying qualities of the XB-70-1 with those simulated on the GPAS during consecutive flights of the two vehicles. In addition, various handling-qualities parameters and time histories for the XB-70 and the airborne simulator were compared to assess simulator fidelity. The GPAS was shown to be capable of accurate and realistic simulation of the XB-70 at two flight conditions (Mach 1.2 at 12,200 meters (40,000 feet) altitude and Mach 2.35 at 16,800 meters (55,000 feet) altitude). In-flight changes to the programed model were required to obtain a satisfactory simulation from the pilot's point of view. In most instances, these changes were necessary to improve model representation of the XB-70 rather than to correct for possible simulator-introduced distortions.

17. Key Words (Suggested by Author(s))	18. Distribution Statement
Airborne simulation Simulation Validation Handling qualities	Unclassified - Unlimited

19. Security Classif. (of this report)	20. Security Classif. (of this page)	21. No. of Pages	22. Price*
Unclassified	Unclassified	70	$3.00

*For sale by the National Technical Information Service, Springfield, Virginia 22151

CONTENTS

Page

INTRODUCTION 1
SYMBOLS 1
GENERAL PURPOSE AIRBORNE SIMULATOR 8
PILOT'S INSTRUMENT PANEL 10
AIRBORNE ANALOG COMPUTER 11
DATA-ACQUISITION SYSTEM 11
VARIABLE FEEL SYSTEM 13
XB-70 AIRPLANE 13
EXPERIMENTAL PROCEDURES 13
SELECTION OF VALIDATION VEHICLE AND FLIGHT CONDITIONS 15
XB-70 MODELING 15
EVALUATION AND COMPARISON METHODS 17
Use of Rating Scales 17
Identification of Discrepancies 19
GPAS SIMULATION OF XB-70 AT MACH 1.2 20
XB-70 FLIGHT 1-63 20
PRIMARY GPAS VALIDATION FLIGHT (45) 23
Simulation of Feel System Characteristics 23
Simulation of Lateral-Directional Characteristics 25
Simulation of Longitudinal Characteristics 28
ANALYSIS OF XB-70 FLIGHT 1-63 AND COMPARISON WITH RESULTS OF GPAS FLIGHT 45 28
Longitudinal 28
Lateral-Directional 31
Comparison of Stability Derivatives and Dynamic Characteristics 33
Further Time-History Comparisons 36
Conclusions on the Validation With the XB-70 at Mach 1.2 37
GPAS SIMULATION OF XB-70 AT MACH 2.35 40
XB-70 FLIGHT 1-68 40
PRIMARY GPAS VALIDATION FLIGHT (54) 40
Simulation of Feel-System Characteristics 40
Simulation of Lateral-Directional Characteristics 42
Simulation of Longitudinal Characteristics 46
ANALYSIS OF XB-70 FLIGHT 1-68 AND COMPARISON WITH RESULTS OF GPAS FLIGHT 54 47
Longitudinal 48
Lateral-Directional 50
Comparison of Stability Derivatives and Dynamic Characteristics 50
Additional Analysis of Feel-System Discrepancies 57
Conclusions on the Validation With the XB-70 at Mach 2.35 58
CONCLUDING REMARKS 58
APPENDIX A - EQUATIONS OF MOTION PROGRAMED ON AN AIRBORNE ANALOG COMPUTER 60
APPENDIX B - SUMMARY OF PILOT COMMENTS ON XB-70 FLIGHT 1-63 61

APPENDIX C - FLIGHT PLAN FOR VALIDATION PORTION OF GPAS FLIGHT 45 62
APPENDIX D - PILOT QUESTIONNAIRE FOR HANDLING-QUALITIES EVALUATION OF XB-70 AND GPAS 64
APPENDIX E - PILOT'S REPORT AND COMMENTS ON XB-70 FLIGHT 1-68 65
APPENDIX F - FLIGHT PLAN FOR GPAS FLIGHT 54 67
APPENDIX G - PILOT B COMMENTS ON LONGITUDINAL SHORT-PERIOD SIMULATION OF XB-70 AT MACH 2.35 (GPAS FLIGHT 54) 69
REFERENCES 70

VALIDATION OF A GENERAL PURPOSE AIRBORNE SIMULATOR FOR SIMULATION OF LARGE TRANSPORT AIRCRAFT HANDLING QUALITIES

By Kenneth J. Szalai
Flight Research Center

INTRODUCTION

Before any simulator can be used confidently as a tool in handling-qualities research, it must be validated. The validation processes may take many forms, but all have one goal: to show that the simulator can be used in lieu of the actual vehicle. The general purpose airborne simulator (GPAS) is a Lockheed JetStar airplane which has been modified to be used as an in-flight simulator for research into the handling qualities of large subsonic and supersonic transport aircraft in cruise (refs. 1 to 4). Thus, validating the GPAS meant demonstrating that a large, high-speed aircraft, the XB-70-1, could be simulated both accurately and realistically. In theory, an accurate simulation would automatically produce a realistic simulation, if accuracy is considered to be reproduction of all the environmental and dynamic responses of a particular aircraft. In practice, however, limitations in physical capability, time, or funds lead to compromises which result in selecting those items which will be duplicated precisely and those which will be reproduced grossly or left entirely uncontrolled. Failure to duplicate a particular parameter or characteristic of a vehicle is justified if the pilot is insensitive to changes in the parameter or characteristic in the actual vehicle. Because it is rarely possible to conduct sensitivity studies on the actual vehicle prior to a simulation program, compromises must be based on previous experience, pilot comments, and sensitivity studies in the simulator.

If the resulting simulation is realistic from the pilot's standpoint, the experimenter is correctly led to assume that the mathematical modeling of the vehicle has been adequate and that the effect of mismatched characteristics on the overall simulation fidelity is slight. The usual simulation result is that several discrepancies exist between the simulator and the actual vehicle. The problem is complicated because it is necessary to determine whether the discrepancies are caused by an inadequate or inaccurate model or mismatched characteristics. This report considers the first possibility, that differences noted by the pilot between the XB-70 and GPAS handling qualities were the result of an inaccurate model of the XB-70. Reference 5 discusses the second possibility, with emphasis on motion cue mismatches which occurred during the validation.

SYMBOLS

Physical quantities in this report are given in the International System of Units (SI) and parenthetically in U.S. Customary Units. The measurements were taken in

the U.S. Customary Units. Factors relating the two systems are presented in reference 6.

b wing span, m (ft)

C_D drag coefficient

$$C_{D_\alpha} = \frac{\partial C_D}{\partial \alpha}$$

$$C_{D_V} = \frac{\partial C_D}{\partial V}$$

C_L lift coefficient

$$C_{L_\alpha} = \frac{\partial C_L}{\partial \alpha}$$

$$C_{L_{\delta_e}} = \frac{\partial C_L}{\partial \delta_e}$$

C_l rolling-moment coefficient

$$C_{l_p} = \frac{\partial C_l}{\partial \left(\frac{pb}{2V_T}\right)}$$

$$C_{l_r} = \frac{\partial C_l}{\partial \left(\frac{rb}{2V_T}\right)}$$

$$C_{l_\beta} = \frac{\partial C_l}{\partial \beta}$$

$$C_{l_{\delta_a}} = \frac{\partial C_l}{\partial \delta_a}$$

$$C_{l_{\delta_r}} = \frac{\partial C_l}{\partial \delta_r}$$

C_m pitching-moment coefficient

$$C_{m_q} = \frac{\partial C_m}{\partial \left(\frac{q\bar{c}}{2V_T}\right)}$$

$C_{m_\alpha} = \frac{\partial C_m}{\partial \alpha}$

$C_{m_{\dot{\alpha}}} = \frac{\partial C_m}{\partial \left(\frac{\dot{\alpha}\bar{c}}{2V_T}\right)}$

$C_{m_{\delta_e}} = \frac{\partial C_m}{\partial \delta_e}$

C_n yawing-moment coefficient

$C_{n_p} = \frac{\partial C_n}{\partial \left(\frac{pb}{2V_T}\right)}$

$C_{n_r} = \frac{\partial C_n}{\partial \left(\frac{rb}{2V_T}\right)}$

$C_{n_\beta} = \frac{\partial C_n}{\partial \beta}$

$C_{n_{\delta_a}} = \frac{\partial C_n}{\partial \delta_a}$

$C_{n_{\delta_r}} = \frac{\partial C_n}{\partial \delta_r}$

C_T thrust coefficient

$C_{T_V} = \frac{\partial C_T}{\partial V}$

C_Y side-force coefficient

$C_{Y_p} = \frac{\partial C_Y}{\partial \left(\frac{pb}{2V_T}\right)}$

$C_{Y_r} = \frac{\partial C_Y}{\partial \left(\frac{rb}{2V_T}\right)}$

$C_{Y_\beta} = \frac{\partial C_Y}{\partial \beta}$

$C_{Y_{\delta_a}} = \frac{\partial C_Y}{\partial \delta_a}$

$C_{Y_{\delta_r}} = \frac{\partial C_Y}{\partial \delta_r}$

$\bar{c}$ mean aerodynamic chord, m (ft)

$D = \bar{q}SC_D$

$D_V = \frac{1}{m}\left(\frac{\partial D}{\partial V} - \frac{\partial T}{\partial V}\right)$

$D_\alpha = \frac{1}{mV_T}\left(\frac{\partial D}{\partial \alpha} + \alpha_T T - mg\right)$

F_a pilot-applied aileron force, N (lb)

F_e pilot-applied elevator force, N (lb)

F_r pilot-applied rudder force, N (lb)

g acceleration of gravity, m/sec^2 (ft/sec^2)

h altitude, m (ft)

I_{XX}, I_{YY}, I_{ZZ} moments of inertia referred to X-, Y-, Z-body axes, respectively, kg-m^2 (slug-ft^2)

I_{XZ} cross product of inertia, referred to X- and Z-body axes, kg-m^2 (slug-ft^2)

$L = \bar{q}SC_L$

$L_p = \frac{\bar{q}Sb}{I_{XX}} \frac{b}{2V_T} C_{l_p}$

$L_r = \frac{\bar{q}Sb}{I_{XX}} \frac{b}{2V_T} C_{l_r}$

$L_\beta = \frac{\bar{q}Sb}{I_{XX}} C_{l_\beta}$

$L_{\delta_a} = \frac{\bar{q}Sb}{I_{XX}} C_{l_{\delta_a}}$

$L_{\delta_r} = \frac{\bar{q}Sb}{I_{XX}} C_{l_{\delta_r}}$

M Mach number

$M_q = \frac{\bar{q}S\bar{c}}{I_{YY}} \frac{\bar{c}}{2V_T} C_{m_q}$

$M_\alpha = \frac{\bar{q}S\bar{c}}{I_{YY}} C_{m_\alpha}$

$M_{\dot{\alpha}} = \frac{\bar{q}S\bar{c}}{I_{YY}} \frac{\bar{c}}{2V_T} C_{m_{\dot{\alpha}}}$

$M_{\Delta T} = \frac{z_T}{I_{YY}}$

$M_{\delta_e} = \frac{\bar{q}S\bar{c}}{I_{YY}} C_{m_{\delta_e}}$

m mass, slugs

$N_p = \frac{\bar{q}Sb}{I_{ZZ}} \frac{b}{2V_T} C_{n_p}$

$N_r = \frac{\bar{q}Sb}{I_{ZZ}} \frac{b}{2V_T} C_{n_r}$

$N_\beta = \frac{\bar{q}Sb}{I_{ZZ}} C_{n_\beta}$

$N_{\delta_a} = \frac{\bar{q}Sb}{I_{ZZ}} C_{n_{\delta_a}}$

$N_{\delta_r} = \frac{\bar{q}Sb}{I_{ZZ}} C_{n_{\delta_r}}$

n_x acceleration of aircraft center of gravity along X-axis, g

n_{y_p} acceleration at pilot's location along Y-axis, g

n_z acceleration of aircraft center of gravity along Z-axis, g

n_{z_p} acceleration at pilot's location along Z-axis, g

n_{z_α}	normal acceleration change per unit change in angle of attack, g/rad
p	rolling angular velocity, deg/sec
p_{ss}	steady-state rolling angular velocity, deg/sec/deg aileron
q	pitching angular velocity, deg/sec
$\bar{q}$	dynamic pressure, $\frac{1}{2}\rho V^2$, N/m^2 (lb/ft^2)
r	yawing angular velocity, deg/sec
S	reference wing area, m^2 (ft^2)
s	Laplace transform variable
T	thrust, N (lb), or period, sec
t	time, sec
V	true airspeed, m/sec (ft/sec)
X, Y, Z	coordinate-system axes (X, wind, positive forward; Y, body, positive toward right wing; Z, body, positive downward)

$$Y_\beta = \frac{\bar{q}S}{mV_T} C_{Y_\beta}$$

$$Y_{\delta_r} = \frac{\bar{q}S}{mV_T} C_{Y_{\delta_r}}$$

$$Z_\alpha = -\frac{1}{mV_T}\left(\frac{\partial L}{\partial \alpha} + \alpha_T \frac{\partial D}{\partial \alpha}\right)$$

$$Z_{\delta_e} = -\frac{1}{mV_T}\frac{\partial L}{\partial \delta_e}$$

$$Z_\theta = -\frac{\alpha_T g}{V_T}$$

z	thrust moment arm about center of gravity
α	angle of attack, deg
β	angle of sideslip, deg
Δ	incremental change

δ_a	total aileron deflection, $\delta_{a_{left}} - \delta_{a_{right}}$, positive for left aileron trailing edge down, deg
δ_{a_p}	pilot's aileron command, positive when commanding positive δ_a, deg
δ_e	elevator deflection, positive trailing edge down, deg
δ_{e_p}	pilot's elevator command, positive when commanding positive δ_e, deg
δ_r	rudder deflection, positive trailing edge left, deg
δ_{r_p}	pilot's rudder command, positive when commanding positive δ_r, deg
ϵ	error signal
ζ	damping ratio
θ	pitch angle, deg
ρ	mass density of air, kg/m^3 (slugs/ft^3)
τ_r	roll-mode time constant, sec
τ_s	spiral-mode time constant, sec
φ	roll angle, deg
ω	frequency, rad/sec or Hz
ω_{sp}	short-period undamped natural frequency, rad/sec
ω_φ	$\frac{\varphi}{\delta_a}(s)$ transfer-function numerator parameter
ω_ψ	Dutch roll mode undamped natural frequency, rad/sec

Special notation:

$\frac{F_e}{n_z}$	stick force per g, N/g (lb/g)
(s)	function of Laplace variable

$\frac{\alpha_c}{\alpha_m}, \frac{\dot{\alpha}_c}{\dot{\alpha}_m}$	input gains to model-controlled system
$\frac{\delta_{e_c}}{\epsilon_\alpha}, \frac{\delta_{e_c}}{\epsilon_{\dot{\alpha}}}$	loop gains of model-controlled system
$\left\lvert \frac{\varphi}{\beta}(s) \right\rvert_\psi$	ratio of bank angle to sideslip angle at Dutch roll frequency
$\frac{\omega_\varphi}{\omega_\psi}$	handling-qualities parameter

Subscripts:

c	command, usually to an actuator
J	JetStar
m	model, analog computer quantity
P	phugoid mode quantity
p	pilot
v	vane
T	trim value
α	pertaining to angle of attack
ψ	pertaining to Dutch roll

GENERAL PURPOSE AIRBORNE SIMULATOR

The GPAS was designed and fabricated by the Cornell Aeronautical Laboratory under NASA contract. A sketch of the layout of GPAS systems in the JetStar is shown in figure 1. The GPAS uses the model-controlled-system (MCS) form of simulation. A simplified block diagram of the principal components of a typical MCS channel is shown in figure 2. The pilot's control inputs are routed to the airborne analog computer by means of an artificial feel system. The computer is programed with the equations of motion and aerodynamic characteristics of the aircraft configuration to be simulated, and selected response variables of the programed configuration (model) are fed to the model-following control system of the GPAS. In figure 2 the variable is model angle of attack α_m. The input gain $\frac{\alpha_c}{\alpha_m}$ is used to compensate for any

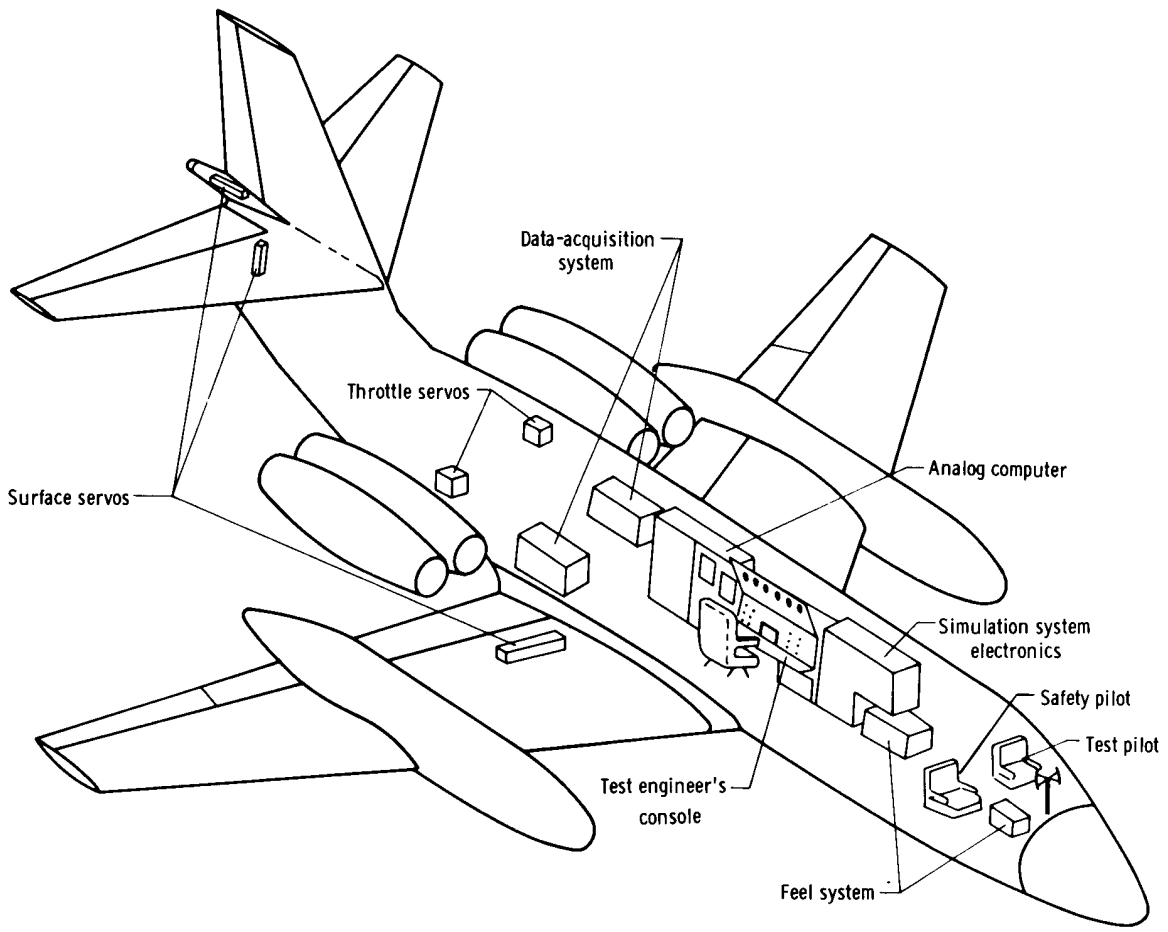

Figure 1. Layout of GPAS systems in the JetStar.

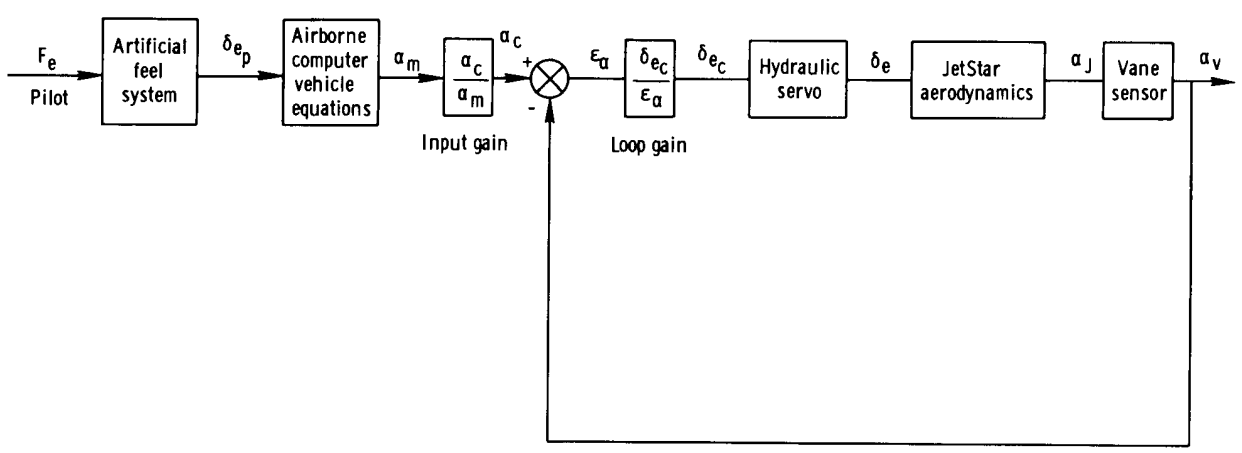

Figure 2. Block diagram of typical model-controlled-system channel.

amplitude errors which might exist in the control system. Model and JetStar angle of attack are compared, and an error signal ϵ_α is generated. This error signal commands a servo through the loop gain $\frac{\delta_{e_c}}{\epsilon_\alpha}$ to drive the elevator surface in a direction to reduce ϵ_α. With a sufficiently high loop gain, ϵ_α is small and the JetStar is forced to reproduce angle-of-attack variations of the model.

In practice, the α loop is not used alone. Another feedback loop, using $\dot{\alpha}$, is added to provide adequate closed-loop JetStar damping. A block diagram of such a configuration, which was used during the GPAS validation program for the longitudinal simulation, is shown in figure 3.

The advantages of the model-controlled system over the more conventional response feedback system, which uses feedback loops to augment basic aircraft stability derivatives, consist primarily of greatly reduced in-flight calibration time and relative insensitivity to variations in base aircraft weight, inertia, and aerodynamic characteristics. For example, model-following fidelity remains fairly constant during a GPAS flight even as fuel is burned.

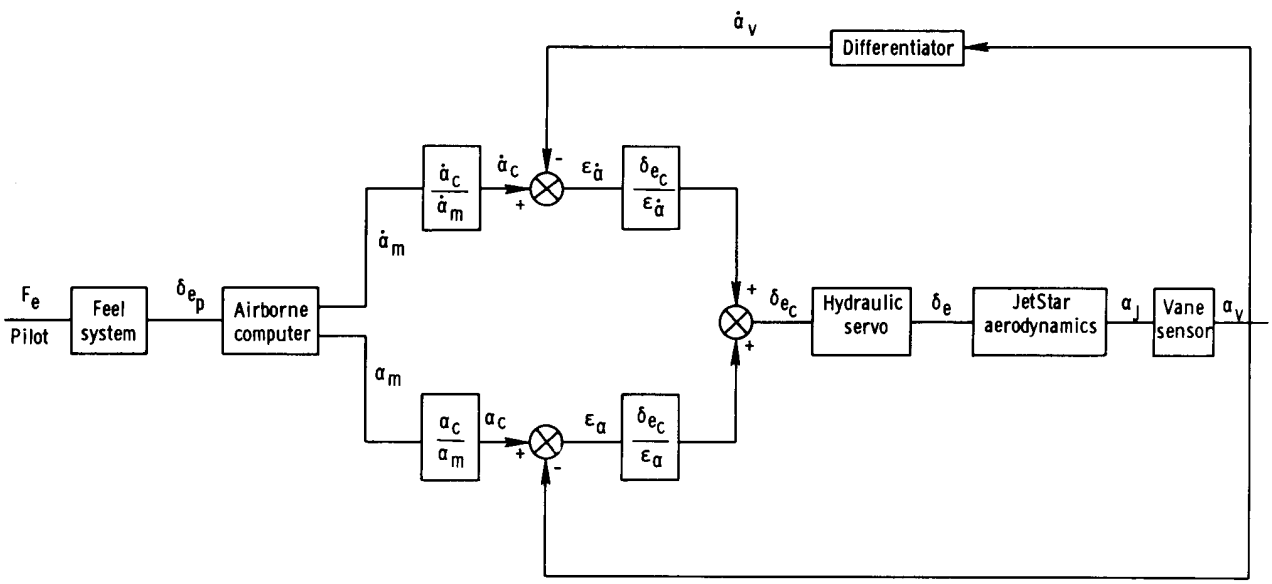

Figure 3. Block diagram of two-loop configuration of model-controlled system used during GPAS validation program for simulating longitudinal short-period dynamics.

In this validation program, α and $\dot{\alpha}$ were followed in the longitudinal mode, and β, $\dot{\beta}$, φ, and p were followed in the lateral-directional mode. No direct acceleration-following loops were used.

PILOT'S INSTRUMENT PANEL

The left-hand pilot's station in the JetStar has been modified to be the simulation station. The instrument panel contains simulated aircraft instruments which were

driven from the onboard analog computer in this program. A photograph of the panel used for the validation program is shown in figure 4. No attempt was made to duplicate

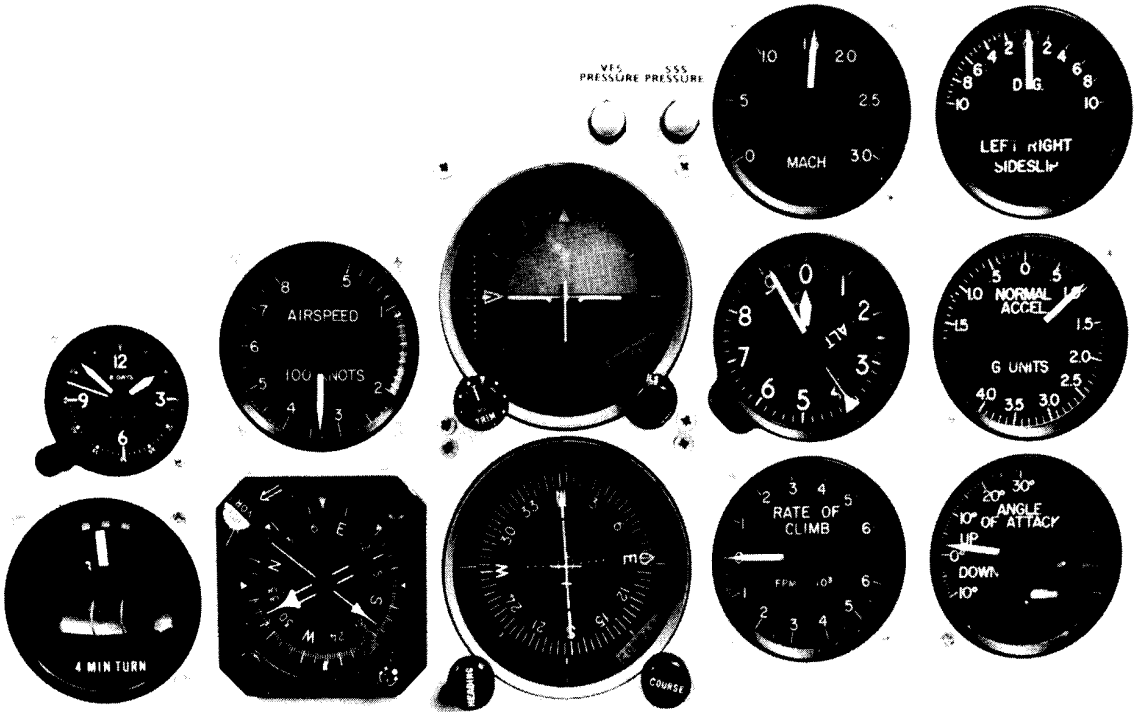

Figure 4. GPAS pilot's instrument panel used during the validation program. *E-19481*

the XB-70 pilot's instrument panel (fig. 5). For most of the GPAS evaluations, the pilots relied on the roll attitude, sideslip, and heading instruments, which were sufficiently similar to their XB-70 counterparts that exact duplication was not considered to be necessary. On the GPAS panel, all instruments were driven from the computer except the gravity ball slip indicator, radio compass, and clock.

AIRBORNE ANALOG COMPUTER

The airborne analog computer on the JetStar was used to represent the XB-70 aerodynamic characteristics, as well as to scale the pilot's instruments. The computer is a 10-volt reference system containing 112 operational amplifiers, 11 integrators, 100 potentiometers, and several nonlinear computing elements. It has a removable, patchable program board and can be operated independently of the motion system, if desired.

DATA-ACQUISITION SYSTEM

Approximately 50 different parameters were recorded on a typical GPAS flight.

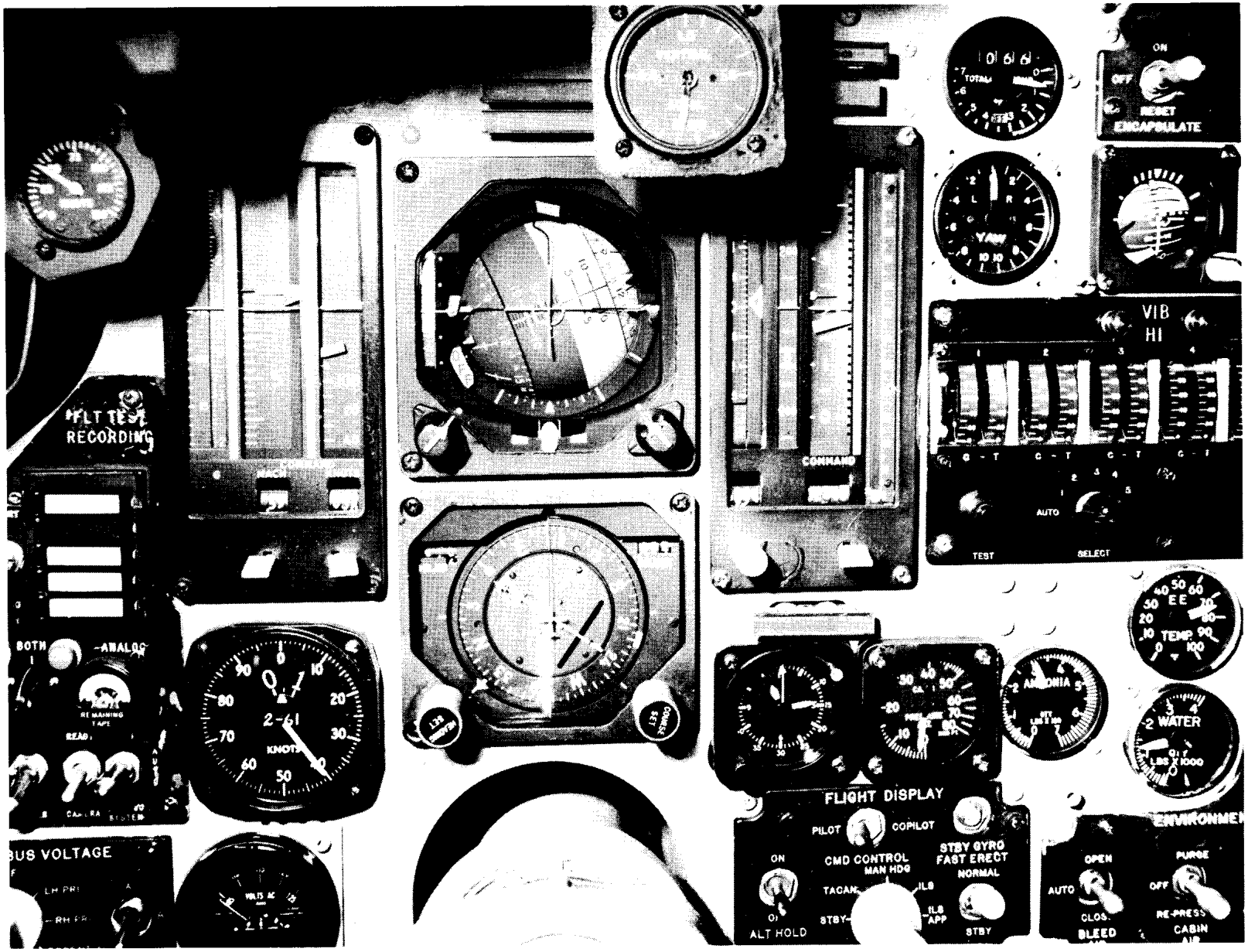

E-19530

Figure 5. XB-70 pilot's instrument panel.

These included analog computer and JetStar responses, as well as pilot control inputs and selected MCS parameters for occasional troubleshooting. Two 50-channel oscillographs were used for in-flight data recording. Some parameters were recorded more than once, with different scale factors, resulting in approximately 65 active channels of recording. A 12-channel direct-writing oscillograph was also available for in-flight monitoring and preflight checks. A voice tape recorder, keyed by the pilot's intercommunication system switch, was used to record all pilot comments and communications with test engineers.

VARIABLE FEEL SYSTEM

The GPAS artificial feel system is an electrohydraulic control system. Applied pilot force is detected by strain gages which in turn command hydraulic servos to move the control to the position corresponding to the applied force. The control position is a function of preselected force gradients and nonlinearities, including dead-band, hysteresis, and breakout force, which are controllable from the test engineer's console.

XB-70 AIRPLANE

The XB-70 is a large, high-speed research airplane with a design gross weight in excess of 227,000 kilograms (500,000 pounds) and a design cruise speed of Mach 3.0 at 21,300 meters (70,000 feet) altitude. It has a thin, low-aspect-ratio, highly swept delta wing, folding wing tips (down), twin movable vertical stabilizers, elevon surfaces for pitch and roll control, a movable canard with trailing-edge flaps, and twin inlets enclosed in the fuselage. Propulsion is provided by six YJ93-GE-3 engines, which each have a 133,000-newton (30,000-pound) thrust classification at sea level. Sketches of the XB-70 and JetStar vehicles, drawn approximately to scale, are shown in figure 6.

The primary XB-70 flight control system consists of irreversible, hydraulic-powered surfaces. Column, wheel, and rudder-pedal controls are provided for the pilot and the copilot. In the pitch system, artificial feel is modulated by a dynamic-pressure bellows with contributing feel from a spring, a hydraulic damper, and a bobweight. In the roll and yaw systems, spring feel bungees are provided. Because the XB-70 was to be simulated at two discrete flight conditions, with only small perturbations around these conditions, the pitch feel system was modeled with fixed characteristics at each flight condition.

EXPERIMENTAL PROCEDURES

The primary goal of the validation program was to show that the GPAS could accurately and realistically simulate a large jet aircraft. In addition, because discrepancies between the GPAS and the simulated vehicle were expected, it was necessary

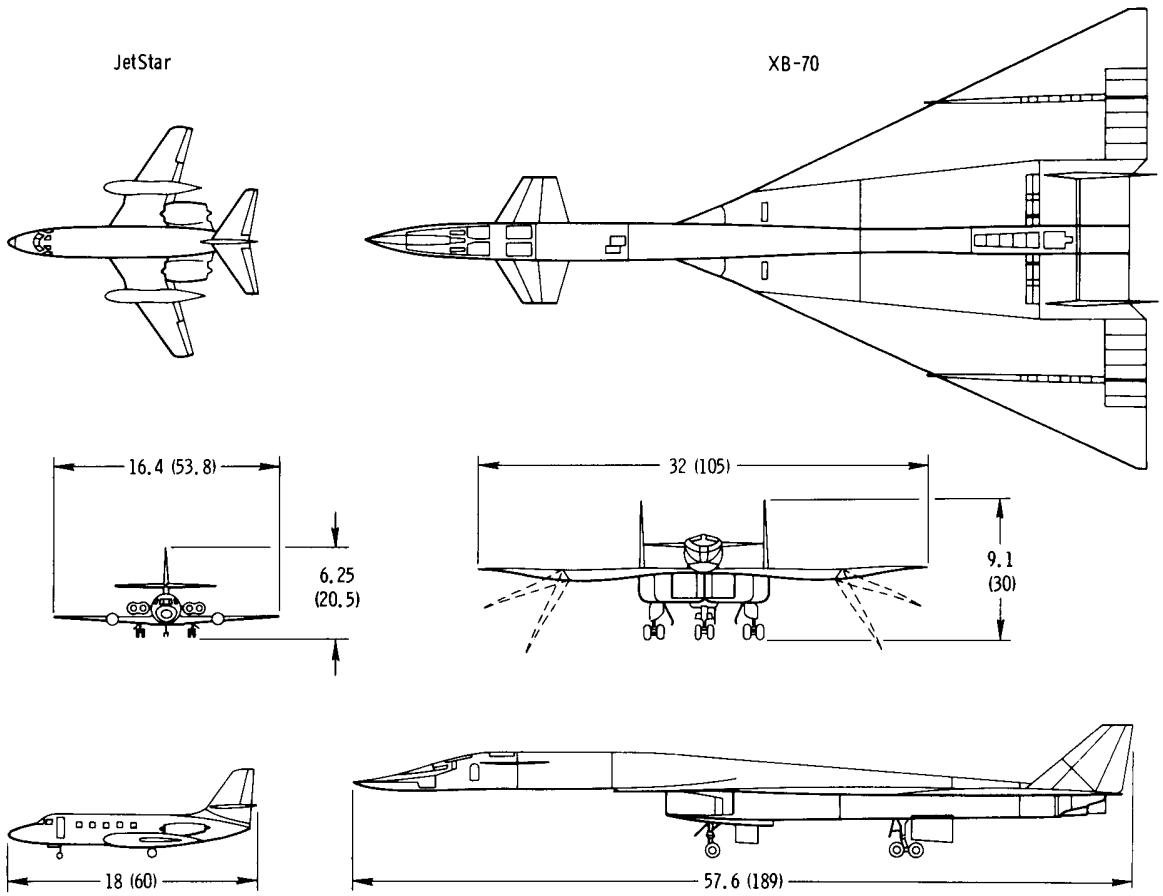

Figure 6. Dimensions (in meters (feet)) of JetStar and XB-70.

to identify the cause of the discrepancies as either modeling inaccuracies or simulator limitations. The program procedures were as follows:

(1) Select the aircraft and flight conditions to simulate.

(2) Model the desired aircraft.

(3) Select the simulator mechanization which reproduced model characteristics thought to be most critical to a satisfactory simulation.

(4) Verify that the simulator performance was as expected in reproducing the selected model characteristics.

(5) Compare the simulator and the actual vehicle characteristics by means of pilot evaluations and time-history comparisons.

(6) Identify the discrepancies and reevaluate the modeling techniques and simulation compromises on the basis of these discrepancies.

SELECTION OF VALIDATION VEHICLE AND FLIGHT CONDITIONS

Although a subsonic jet transport could have been used as the validation vehicle for the GPAS to simulate, the XB-70 was chosen for the following reasons:

(1) Supersonic transport studies were expected to be emphasized on the GPAS, and the XB-70 was the only large supersonic vehicle flying at the time the validation program was started.

(2) The Flight Research Center was expending considerable effort to obtain aerodynamic stability derivatives for the XB-70 during the flight-test program, thus reasonably good flight data were available.

(3) The ratios of pitch-to-roll and yaw-to-roll inertias and the pilot-to-center-of-gravity distance of the XB-70 are similar to those of proposed supersonic transport configurations.

(4) Both NASA and U.S. Air Force XB-70 pilots were available to fly GPAS simulations of the XB-70.

Lateral-directional dynamics were emphasized over the longitudinal dynamics for two reasons: (1) Lateral-directional dynamics are a more severe test of simulator capability with the model coupling and (2) the more critical XB-70 handling-qualities problems were in the lateral-directional area, thus GPAS results in this area would be useful in assessing possible methods of alleviating the problems.

The two XB-70 flight conditions chosen for simulation were: (1) Mach 1.2 at 12,200 meters (40,000 feet) altitude with wing tips half down (25°) and (2) Mach 2.35 at 16,800 meters (55,000 feet) altitude with wing tips full down (65°). The Mach 1.2 condition had moderate adverse yaw due to aileron, positive dihedral, and an $\frac{\omega_\varphi}{\omega_\psi}$ ratio less than 1. The Mach 2.35 condition also had adverse yaw but negative dihedral and an $\frac{\omega_\varphi}{\omega_\psi}$ ratio greater than 1, with the resulting pilot-induced-oscillation (PIO) tendency. The longitudinal short-period dynamics of both flight conditions were moderately damped and displayed no unusual characteristics. These dynamic characteristics are those exhibited by the XB-70 with no stability augmentation. The two flight conditions are representative of many data points in the XB-70 flight envelope but present sufficient contrasts to represent a fairly broad range of dynamics. The JetStar was flown at a nominal flight condition of 250 knots indicated airspeed at 6096 meters (20,000 feet) altitude.

XB-70 MODELING

With few exceptions, only aerodynamic data obtained in actual flight tests were used in the airborne analog computer program. Aerodynamic stability derivatives (ref. 7) were obtained by analog matching specially conditioned XB-70 time histories. This process yielded constant coefficients. The analog computer was programed with

two uncoupled sets of three-degree-of-freedom linear perturbation equations (appendix A). It was of interest to determine if such a set of equations would be acceptable for an airborne simulation of this type. In practice, the uncoupled equations did not cause many problems because of the generally mild maneuvers performed with the simulated XB-70 vehicle; although, when steep turns ($\varphi > 30°$) were performed occasionally, the uncoupled equations proved to be unacceptable. These were the only circumstances that prompted pilot awareness of the uncoupled nature of the simulator. For typical cruise maneuvering with bank angles less than approximately 20°, the uncoupled equations were adequate.

Another problem associated with modeling the XB-70 concerned the control system. Experience with the GPAS showed that time lags due to model-following were from 0.05 second to 0.4 second, depending on the loop gains used and the model characteristics. Unless model-following could be accomplished with virtually no lag, it was apparent that the modeling of XB-70 control-system dynamics would only add additional, undesirable lags in the overall following path from pilot to JetStar response. It was decided that the control-system dynamics of the XB-70 would not be included in the analog model. Rather, the assumption was made (and verified in later examinations) that the time lags associated with the GPAS model-following system are comparable (within 0.1 second to 0.2 second near XB-70 natural frequencies) to the lags in the XB-70 control path from pilot control motion to vehicle response (fig. 7). The two block diagrams in figure 7 represent the flow of the control signal from pilot to vehicle

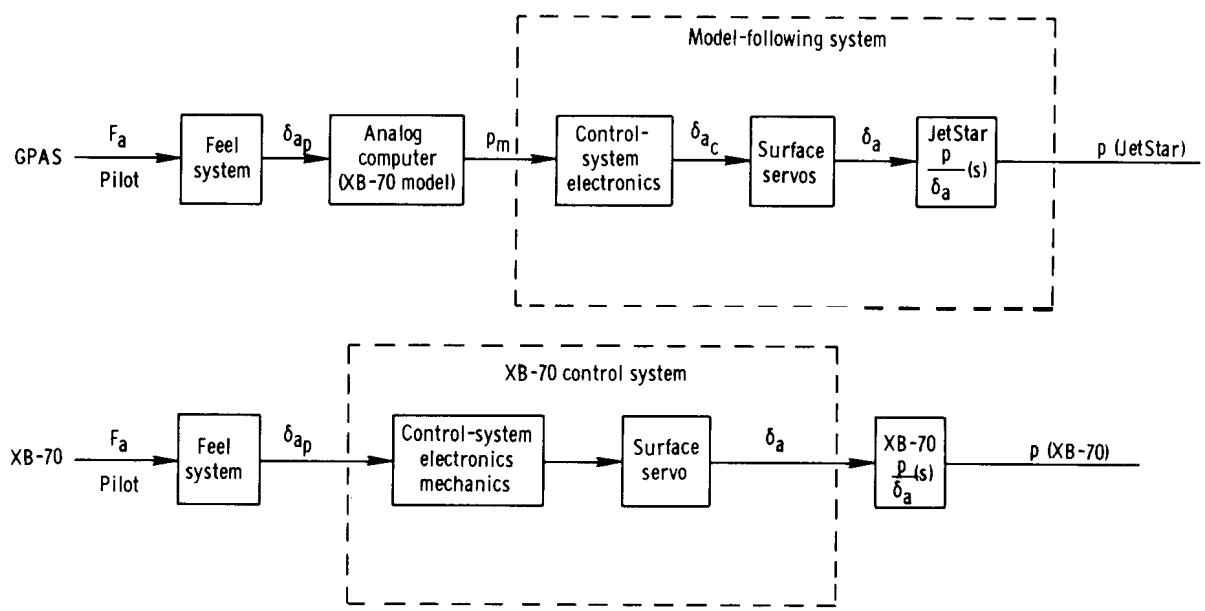

Figure 7. Comparison of GPAS and XB-70 roll-control paths.

response. Roll rate is selected as an example. The analog computer is programed to represent only the aerodynamic portion of the XB-70 model, the block labeled "XB-70 $\frac{p}{\delta_a}(s)$." The two systems enclosed in dashed lines were assumed to have similar frequency-response characteristics. Thus, if the two feel systems have the

same dynamics, the lag between a pilot control input and the resulting aircraft motion will be the same for the GPAS and the XB-70. From comparisons of XB-70 and GPAS responses for identical pilot inputs, it was determined that the systems enclosed by the dashed lines were similar. However, for total IFR flight, the GPAS instrument-displayed response would not necessarily duplicate the displayed response the pilot would see in the XB-70, because the displayed signals in the GPAS originate in the computer and do not pass through any control-system lags as in the XB-70.

The fairly close match of the GPAS model-following lags and the XB-70 control-system lags was fortunate and would not necessarily exist in future programs. It would be desirable to minimize GPAS model-following lags to near zero before programing the control-system characteristics on the analog computer.

EVALUATION AND COMPARISON METHODS

A block diagram representing the conduct of the validation program is shown in figure 8. Flight tests of the XB-70 yielded pilot comments, ratings, and time histories. The time histories were analog-matched to obtain stability derivatives which were used to program the GPAS. The same pilot then flew the GPAS simulation, and comments, ratings, and time histories were collected. In addition, the pilot rated the simulation fidelity using a special scale developed for the validation program. Thus, pilot comments, ratings, and time histories were available for comparisons.

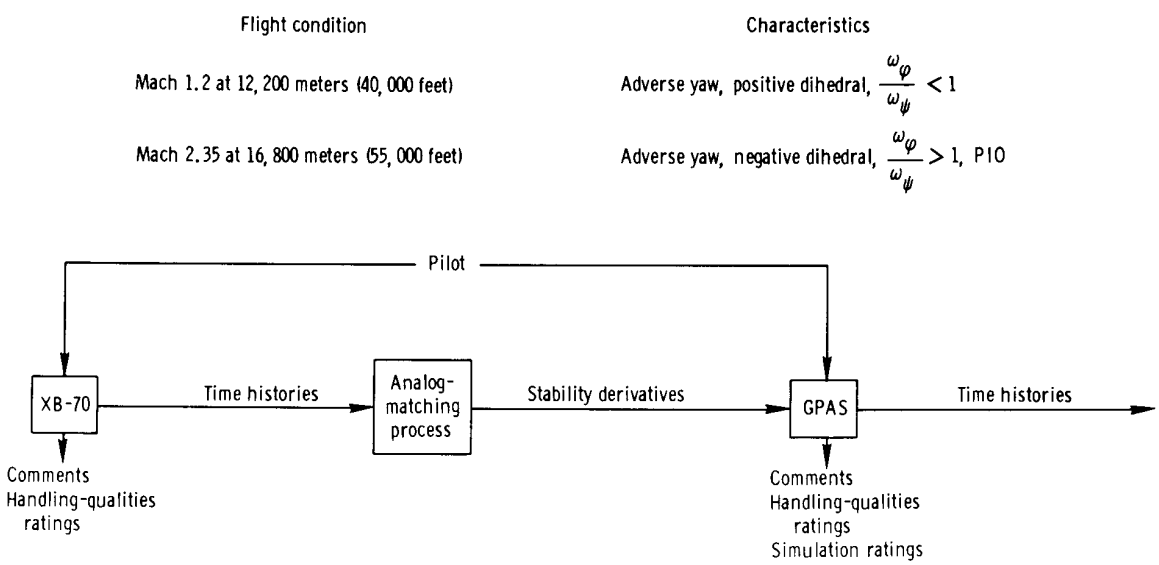

Figure 8. Flow diagram of GPAS validation program.

Use of Rating Scales

One method of determining simulator fidelity is to compare numerical pilot ratings for the simulator handling qualities with those given for the actual vehicle. Figure 9 shows the pilot rating scale used during the GPAS validation program. The scale was

Controllable Capable of being controlled or managed in context of mission, with available pilot attention.	Acceptable May have deficiencies which warrant improvement but adequate for mission. Pilot compensation, if required to achieve acceptable performance, is feasible.	Satisfactory Meets all requirements and expectations. Good enough without improvement. Clearly adequate for mission.	Excellent, highly desirable.	A1
			Good, pleasant, well behaved.	A2
			Fair, some mildly unpleasant characteristics. Good enough for mission without improvement.	A3
		Unsatisfactory Reluctantly acceptable deficiencies which warrant improvement. Performance adequate for mission with feasible pilot compensation.	Some minor but annoying deficiencies. Improvement is requested. Effect on performance is easily compensated for by pilot.	A4
			Moderately objectionable deficiencies. Improvement is needed. Reasonable performance requires considerable pilot compensation.	A5
			Very objectionable deficiencies. Major improvements are needed. Requires best available pilot compensation to achieve acceptable performance.	A6
	Unacceptable Deficiencies which require mandatory improvement. Inadequate performance for mission even with maximum feasible pilot compensation.		Major deficiencies which require mandatory improvement for acceptance. Controllable. Performance inadequate for mission, or pilot compensation required for minimum acceptable performance in mission is too high.	U7
			Controllable with difficulty. Requires substantial pilot skill and attention to retain control and continue mission.	U8
			Marginally controllable in mission. Requires maximum available pilot skill and attention to retain control.	U9
Uncontrollable Control will be lost during some portion of mission			Uncontrollable in mission.	U10

Figure 9. Ames Research Center/Cornell Aeronautical Laboratory revised pilot rating scale.

developed jointly by the NASA Ames Research Center and the Cornell Aeronautical Laboratory (ref. 8).

Another method of assessing the fidelity of a simulator is for the evaluation pilot to assign a numerical rating which represents the degree of fidelity of the simulation. The numerical rating scale developed for the validation program is shown in figure 10. The format is similar to that of the Cornell 10-point scale (ref. 9) in its category and adjective breakdown. The descriptions accompanying each rating are designed to

Category	Rating	Adjective	Description
Satisfactory representation of actual vehicle	1	Excellent	Virtually no discrepancies; simulator reproduces actual vehicle characteristics to the best of my memory. Simulator results directly applicable to actual vehicle with high degree of confidence.
	2	Good	Very minor discrepancies. The simulator comes close to duplicating actual vehicle characteristics. Simulator results in most areas would be applicable to actual vehicle with confidence.
	3	Fair	Simulator is representative of actual vehicle. Some minor discrepancies are noticeable, but not distracting enough to mask primary characteristics. Simulator trends could be applied to actual vehicle.
Unsatisfactory representation of actual vehicle	4	Poor	Simulator needs work. It has many minor discrepancies which are annoying. Simulator would need some improvement before applying results directly to actual vehicle, but is useful for general handling-qualities investigations for this class of aircraft.
	5	Bad	Simulator not representative. Discrepancies exist which prevent actual vehicle characteristics from being recognized. Results obtained here should be considered as unreliable.
	6	Very bad	Possible simulator malfunction. Wrong sign, inoperative controls, other gross discrepancies prevent comparison from even being attempted. No data.

Figure 10. Simulation pilot rating scale developed for use in validation program.

guide the pilot in assigning a rating. In practice the pilots used the scale to rate the overall simulation fidelity, along with specific items such as the feel-system duplication. Both of the XB-70 pilots in this program thought the simulation pilot rating scale was helpful and used it willingly. The scale provides common ground for test pilot and engineer in determining simulator effectiveness. In this report, a simulation pilot rating is referred to as an SPR.

One other rating scale was used, the PIO scale shown in figure 11. This scale, developed by the Cornell Aeronautical Laboratory (ref. 8), was found to be useful during the Mach 2.35 validation flights for standardizing comments pertaining to the PIO conditions encountered.

Description	Numerical rating
No tendency for pilot to induce undesirable motions.	1
Undesirable motions tend to occur when pilot initiates abrupt maneuvers or attempts tight control. These motions can be prevented or eliminated by pilot technique.	2
Undesirable motions easily induced when pilot initiates abrupt maneuvers or attempts tight control. These motions can be prevented or eliminated but only at sacrifice to task performance or through considerable pilot attention and effort.	3
Oscillations tend to develop when pilot initiates abrupt maneuvers or attempts tight control. Pilot must reduce gain or abandon task to recover.	4
Divergent oscillations tend to develop when pilot initiates abrupt maneuvers or attempts tight control. Pilot must open loop by releasing or freezing the stick.	5
Disturbance or normal pilot control may cause divergent oscillation. Pilot must open control loop by releasing or freezing the stick.	6

Figure 11. Pilot-induced-oscillation tendency rating scale.

Identification of Discrepancies

Early attempts to establish the fidelity of the GPAS simulation were only partially successful; comments from XB-70 pilots who had flown the GPAS indicated that there were some discrepancies in the XB-70 simulation. The discrepancies can be categorized as being due to one or more of the following factors: (1) pilot recollection of XB-70 characteristics; (2) ability of the GPAS to reproduce computer-commanded dynamics; and (3) accuracy of aerodynamic stability derivatives used on the airborne computer.

Pilot recollection of XB-70 characteristics. – In comparing early GPAS simulations with the actual XB-70, the XB-70 pilots pointed out the difficulty in remembering two specific flight conditions out of the entire flight envelope. Neither pilot had accumulated much time at either flight condition; therefore, to obtain the detailed critiques of the GPAS that were required, it was necessary to conduct a GPAS simulation flight as soon as practical after an XB-70 flight at the desired flight condition. One of the two primary validation flights on the GPAS was conducted the day after an XB-70 flight and the other, 3 days after an XB-70 flight. The latter proved to be marginally acceptable in terms of time between flights. Table 1 shows the chronological order of pertinent flights in the GPAS validation program.

TABLE 1. – CHRONOLOGICAL SEQUENCE OF FORMAL VALIDATION FLIGHTS

Date	Airplane	Flight number	Actual or simulated flight condition	Purpose of flight
6-2-67	XB-70	1-63	M = 1.2 at 12,192 m (40,000 ft)	Handling-qualities evaluation
6-5-67	GPAS	45	M = 1.2 at 12,192 m (40,000 ft)	Validation of GPAS
10-11-67	XB-70	1-68	M = 2.35 at 16,764 m (55,000 ft)	Handling-qualities evaluation for GPAS
10-12-67	GPAS	54	M = 2.35 at 16,764 m (55,000 ft)	Validation of GPAS
11-13-67	GPAS	59	M = 2.35 at 16,764 m (55,000 ft)	Motion/visual cues

GPAS simulation ability. – Although it had been established early in the GPAS flight checkout program that the JetStar closely followed commanded motions from the computer, the effect of not being able to match exactly all visual and motion cues was not clear. This was investigated as part of the validation program because of the possibility that peculiar simulator characteristics could distort the presentation to the pilot. Reference 5 contains the results of this portion of the study.

Stability-derivative uncertainty. – The first sets of stability derivatives for the two XB-70 flight conditions selected were obtained from weak maneuvers performed early in the XB-70 flight-test program, when the aircraft was being flown in a conservative manner. The inadequate excitation of all the modes degraded the accuracy of the stability derivatives. Therefore, these two flight points were repeated on the XB-70, and more active maneuvers were analog-matched. These flights also served as the first half of the set of validation flights, with the GPAS flown soon after the XB-70 for pilot evaluation.

The time between the set of flights was insufficient to perform the analog-matching and update GPAS analog computer data; thus, changes were made to the stability derivatives during the GPAS flight on the basis of pilot comments on noted discrepancies. It was found that the changes made to the derivatives on the airborne computer were necessary to correct original model data inaccuracy and differences caused by variation in gross weight and center of gravity between the condition set up on the GPAS and the flight condition obtained during the XB-70 flight. Consequently, the resultant GPAS configuration compared favorably with the analog-matching results derived from better conditioned XB-70 maneuvers.

GPAS SIMULATION OF XB-70 AT MACH 1.2

XB-70 FLIGHT 1-63

The XB-70 was flown by pilot A for nearly 20 minutes at Mach 1.2 on June 2, 1967 (flight 1-63). No maneuvers were performed specifically for the GPAS validation. Instead, the following standard set of maneuvers, which had been selected as suitable for analog matching and a handling-qualities evaluation, was used: (1) Pullup and release (to 1.4g), (2) wind-up turn (1.4g), (3) double aileron pulse, (4) double rudder pulse, (5) wings-level sideslip, and (6) lateral-directional maneuver (normal and

faster than normal rolls to 20° bank, change heading 20°; perform coordinated and uncoordinated).

Pilot comments made during the XB-70 flight and at a postflight debriefing are summarized in appendix B. The following comments had the greatest impact on the GPAS simulation:

(1) The nose ramp was up during the Mach 1.2 portion of the flight.

(2) The yaw needle was dead in 3 1/2 cycles.

(3) The adverse yaw due to aileron was light (less than in other flight conditions on the XB-70); 3/4° of sideslip was generated in slow rolls, 1 1/2° in fast rolls.

(4) In a spiral test performed at Mach 1.4 and 9800 meters (32,000 feet) altitude, the spiral-mode stability was weak.

Because the GPAS would be flown VFR, there had been no preparations to simulate the restricted forward vision resulting from the ramp being up. Comments relating to Dutch roll damping indicated that the XB-70 was more heavily damped than the $\zeta_\psi = 0.056$ representation on the GPAS. Measurements taken from telemetry data the day of the XB-70 flight indicated that the damping ratio was greater than 0.1. The adverse-yaw generation apparently surprised the pilot as being relatively light compared with other XB-70 conditions.

The original aerodynamic data for this Mach 1.2 flight condition were obtained by analog-matching a release-from-sideslip maneuver and a pullup and release performed on XB-70 flight 1-5. The aerodynamic data and associated dynamic modes are listed in table 2. Several stability derivatives were checked to assess their influence on the Dutch roll damping and spiral time constant. Both C_{n_r} and C_{l_r} showed significant influence on ζ_ψ, but lower C_{l_r} values also affected the spiral time constant in the desired direction (toward neutral) while it increased the damping. Figure 12 shows this variation of Dutch roll damping and spiral time constant as a function of C_{n_r} and C_{l_r}. It

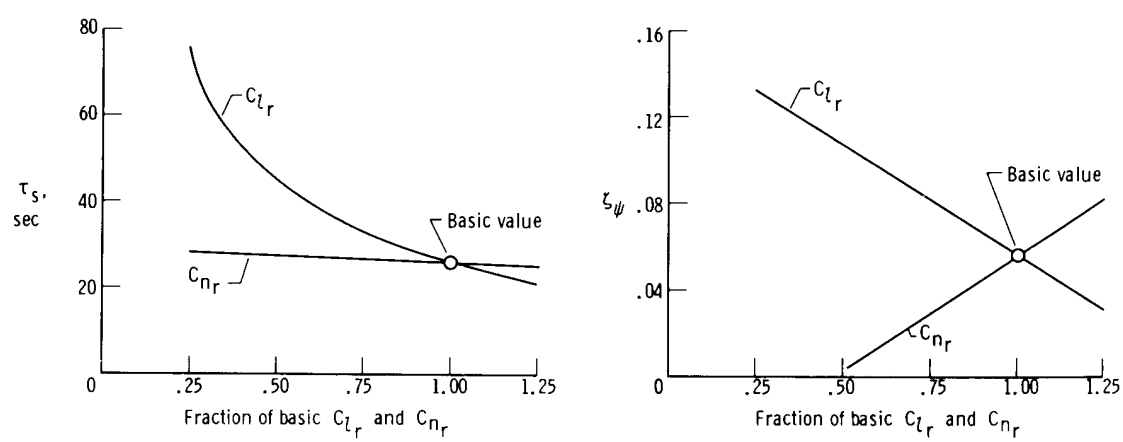

Figure 12. Variation in ζ_ψ and τ_s for fractional changes in C_{n_r} and C_{l_r} using basic Mach 1.2 aerodynamic data from XB-70 flight 1-5.

TABLE 2. – AERODYNAMIC DATA FOR THE XB-70 AT MACH 1.2 AND 12,200 METERS (40,000 FEET) ALTITUDE FROM ANALOG MATCH OF FLIGHT 1-5

Longitudinal:					
Geometric characteristics -					
Gross weight, kg (lb)					140,900 (310,700)
Center of gravity, percent mean aerodynamic chord					21.40
Angle of attack, deg					5.1
True airspeed, m/sec (ft/sec)					354.2 (1162)
Dynamic pressure, N/m^2 (lb/ft^2)					17,700 (369)
I_{YY}, kg-m^2 (slug-ft^2)					22.9×10^6 (16.9×10^6)
Nondimensional stability derivatives (flight data, except those with asterisks), per rad -					
$^*C_{D_V}$	0.0000037	C_{L_α}	2.90	C_{m_α}	-0.337
$^*C_{D_\alpha}$	0.0847	$C_{L_{\delta_e}}$	0.161	$C_{m_{\delta_e}}$	-0.087
$^*C_{T_V}$	0			C_{m_q}	-1.60
Dynamic characteristics -					
ω_{sp}, rad/sec					2.0
ζ_{sp}					0.30
ω_P, rad/sec					0.0347
T_P, sec					181
ζ_P					-0.03
n_{z_α}, g/rad					21.8
Lateral-directional:					
Geometric characteristics -					
Distance from center of gravity to pilot's station, m (ft)					32 (105)
Gross weight, kg (lb)					139,700 (308,000)
Center of gravity, percent mean aerodynamic chord					21.65
Angle of attack, deg					5.3
True airspeed, m/sec (ft/sec)					354 (1160)
Dynamic pressure, N/m^2 (lb/ft^2)					17,700 (370)
I_{XX}, kg-m^2 (slug-ft^2)					1.963×10^6 (1.448×10^6)
I_{ZZ}, kg-m^2 (slug-ft^2)					24.65×10^6 (18.18×10^6)
I_{XZ}, kg-m^2 (slug-ft^2)					-0.864×10^6 (-0.637×10^6)
Nondimensional stability derivatives (flight data), per rad -					
$C_{Y_{\delta_a}}$	0.00264	$C_{l_{\delta_a}}$	0.00991	$C_{n_{\delta_a}}$	-0.00246
$C_{Y_{\delta_r}}$	0.11231	$C_{l_{\delta_r}}$	-0.01232	$C_{n_{\delta_r}}$	-0.06389
C_{Y_r}	0	C_{l_r}	-0.36620	C_{n_r}	-0.46660
C_{Y_β}	-0.38830	C_{l_β}	-0.01266	C_{n_β}	0.09856
C_{Y_p}	0	C_{l_p}	-0.22500	C_{n_p}	-0.18590
Dynamic characteristics -					
ω_ψ, rad/sec					1.29
ζ_ψ					0.056
τ_r, sec					0.56
τ_s, sec					25.9
$\left\lvert \frac{\varphi}{\beta}(s) \right\rvert_\psi$					1.45
Angle $\frac{\varphi}{\beta}(s)_\psi$, deg					1.53
$\frac{\omega_\varphi}{\omega_\psi}$					0.89
p_{ss}, deg/sec/deg					0.738

was noted that a 50-percent reduction in C_{l_r} resulted in a ζ_ψ of 0.107 and a τ_s of 45.3 seconds. The complete dynamics resulting from this change and the original dynamics are listed in table 3. A decrease in C_{l_r} was considered to be the most direct means of correcting the Dutch roll damping and spiral time constant discrepancy expected in the GPAS simulation.

TABLE 3.–ORIGINAL AND REDUCED C_{l_r} DYNAMICS FOR XB-70 MODEL

Parameter	Original data from flight 1-5	C_{l_r} reduced 50 percent
ω_ψ, rad/sec	1.29	1.28
ζ_ψ	0.056	0.107
τ_r, sec	.56	.58
τ_s, sec	25.9	45.3
$\left\lvert\frac{\varphi}{\beta}(s)\right\rvert_\psi$	1.45	1.14
Angle $\frac{\varphi}{\beta}(s)_\psi$, deg	1.53	18.3
$\frac{\omega_\varphi}{\omega_\psi}$	.89	.89
p_{ss}, deg/sec/deg	.738	.772

PRIMARY GPAS VALIDATION FLIGHT (45)

On June 5, 1967, pilot A flew the GPAS simulation of the Mach 1.2 condition for nearly 3 hours. The flight plan for the validation portion of the flight is shown in appendix C.

Simulation of Feel System Characteristics

Pilot A compared the GPAS feel system characteristics with those of the XB-70 and requested some changes.

Elevator. – The GPAS elevator feel system was judged to be representative of that of the XB-70, with no major discrepancies. The pilot stated that the GPAS did not seem to have as much breakout force as the XB-70, but the XB-70 did not have the forceful centering characteristics that the GPAS showed. He assigned the following simulation ratings:

	SPR
Breakout force	3
Force gradient	2

Control cycles for the GPAS and XB-70 elevator feel systems are shown in figure 13.

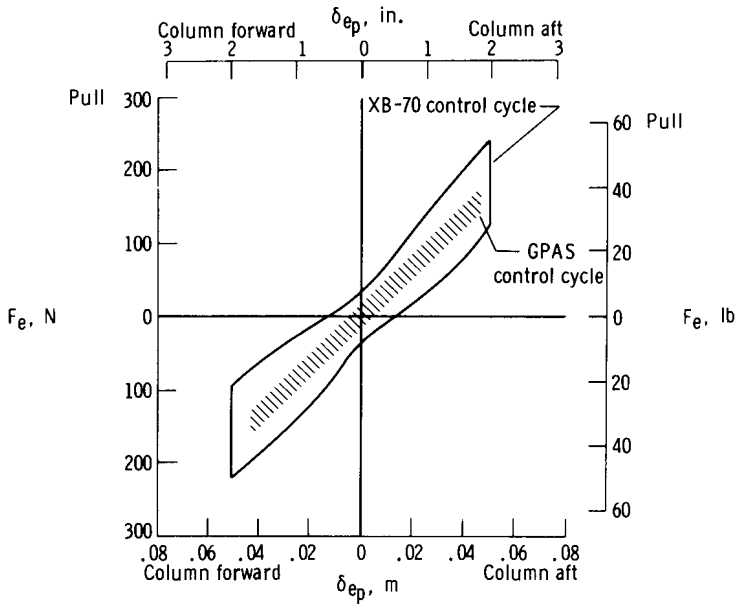

Figure 13. Comparison of static characteristics of GPAS and XB-70 elevator feel systems. Mach 1.2 simulation.

Aileron. – The pilot believed that the programed aileron force gradient of 3.1 N/deg (0.70 lb/deg) was too high, especially in the region around the center position, and requested that the force gradient be decreased to 2.2 N/deg (0.50 lb/deg). XB-70 and final GPAS aileron control cycles are compared in figure 14.

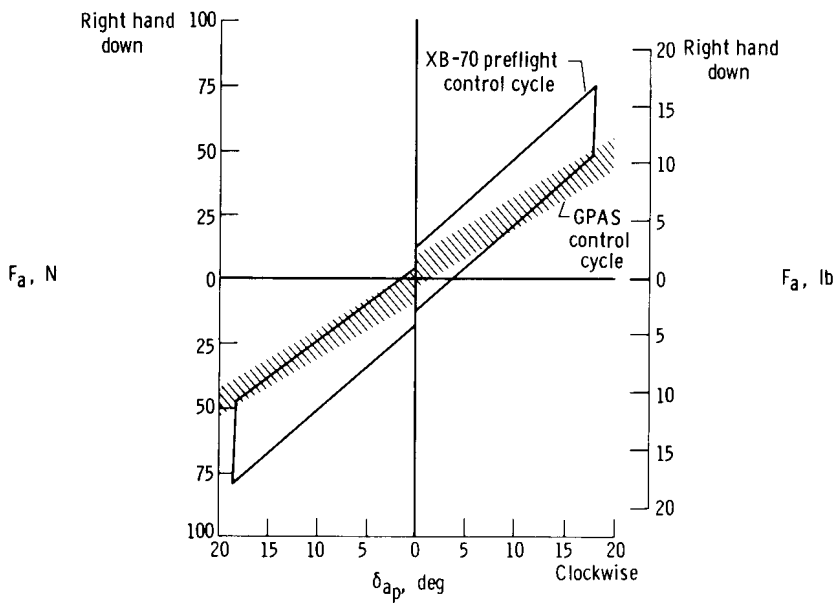

Figure 14. Comparison of static characteristics of XB-70 and GPAS aileron feel systems after flight 45 changes. Mach 1.2 simulation.

Rudder. – The pilot stated that the GPAS rudder feel system felt heavier than the XB-70 system. As a result, the GPAS rudder feel breakout force and gradient were reduced to the point where the pilot believed the XB-70 feel was duplicated. Figure 15 shows the force and displacement characteristics of the XB-70 and the GPAS during control cycles. The original GPAS static feel characteristics appeared to have matched those of the XB-70 well. The final GPAS configuration, which was required to satisfy the pilot, has a lower force gradient than the XB-70 rudder feel system. Further analysis of the GPAS feel system indicated that low bandwidth in the artificial feel system, which led to sluggish response, was the primary reason the pilots considered the GPAS force levels to be too high when they statically matched those of the XB-70 well.

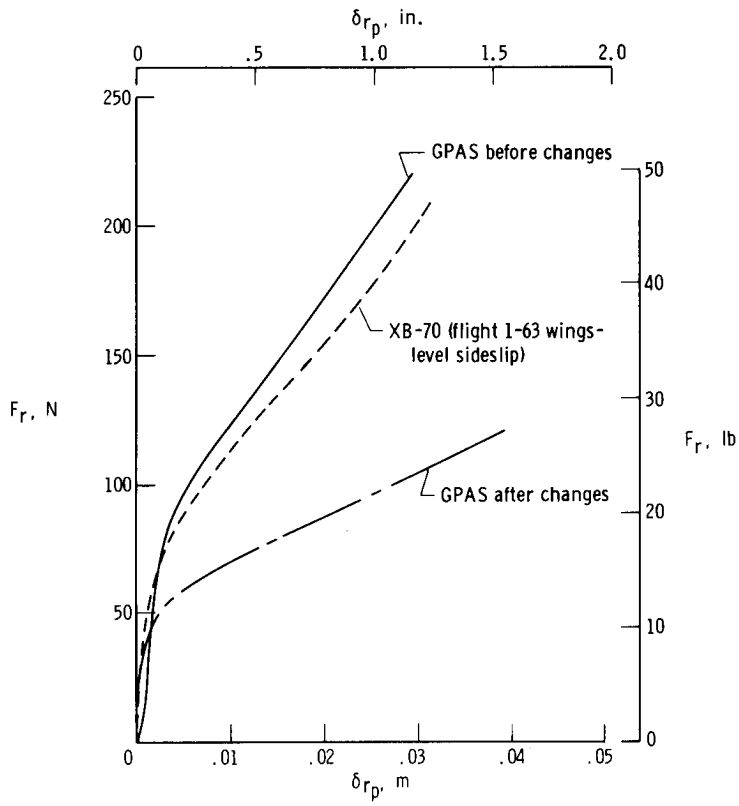

Figure 15. Comparison of static characteristics of XB-70 and GPAS rudder feel systems. Mach 1.2 simulation.

Simulation of Lateral-Directional Characteristics

Pilot comments and ratings of the lateral-directional simulation are summarized in table 4.

Dutch roll damping. – The pilot thought that one of the most significant improvements in the simulation during this flight was in Dutch roll damping. Not much time elapsed before the pilot made strong statements on the GPAS low Dutch roll damping representation; consequently, the derivative C_{l_r} was reduced 50 percent. He considered this one change sufficient to improve the damping representation to a realistic level. The pilot doubted whether he could direct any further changes to improve the damping simulation.

TABLE 4. – SUMMARY OF PILOT A COMMENTS ON GPAS FLIGHT 45
[Mach 1.2 simulation]

Item	SPR	Handling-qualities pilot rating	Comments
Dutch roll damping (before C_{l_r} change)	5	6	Not representative of XB-70. Damping in XB-70 is better by 50 to 60 percent. The simulator seemed to never stop, and that's not like the XB-70.
Dutch roll damping (50 percent of C_{l_r})	2	Good	You have got the Dutch roll damping far more realistic than when we started. Damping is about the same as the airplane's [XB-70]. The airplane behaved like this. I can't get you any closer.
Adverse yaw due to aileron	2	----------	Yaw due to aileron--that's just about like I saw in the XB-70. Response to double aileron pulses, like the airplane. You get about 2° of sideslip.
Roll power	2	Excellent	More roll power than I need. I don't see anything grossly different here. XB-70 may have a little more roll rate, but I know I've got a JetStar in my hands and not a big slab of half an acre of honeycomb. Simulator has excellent roll power.
Roll damping	2	2	Simulation is good. Damping I see here is fine and representative.
Wings-level sideslip	--------	----------	Full rudder gives 3° sideslip. That's what I got in the XB-70. I'm holding 15 to 18° of wheel here. I didn't need that much in the XB-70. (Wheel angle was 4.5° left in XB-70, but trimmed position was 7.5° right. This yields 12° in XB-70.)
Dihedral (roll off with rudder)	2	----------	Looks representative of XB-70. Not real strong.
Spiral mode (after C_{l_r} change)	--------	----------	Still a little stronger than XB-70, but it's representative.
Lateral-directional maneuver (after C_{l_r} change)	--------	----------	Representative of XB-70. It doesn't pay to coordinate for that heading change. Precise heading changes like the XB-70. Get 3/4° sideslip for slow rolls, 1 1/2° for fast rolls; same as XB-70.
Side force	--------	----------	Can't feel any in the XB-70. Can't feel much here. It takes about 4° of sideslip here before I can feel anything.
Overall lateral-directional	5 Original 2 Final	6 Original 2 Final	I think the simulation is pretty good. It didn't start out that way. I think we've made a tremendous improvement in the aileron feel and Dutch roll dynamics.

During the postflight discussion, the pilot expressed some concern that the outside visual cues on the GPAS aided him in detecting the low damping. He questioned whether the XB-70 might have appeared less damped had the nose ramp been down. Later in the XB-70 flight-test program, he had an opportunity to observe the damping characteristics at this flight condition with the nose ramp down. His impression of Dutch roll damping was unchanged from that with the ramp up.

The lateral-directional dynamic response of the original configuration and that corresponding to a 50-percent reduction in C_{l_r} are compared in figure 16. As shown, the change in Dutch roll damping is the only significant result of the C_{l_r} reduction.

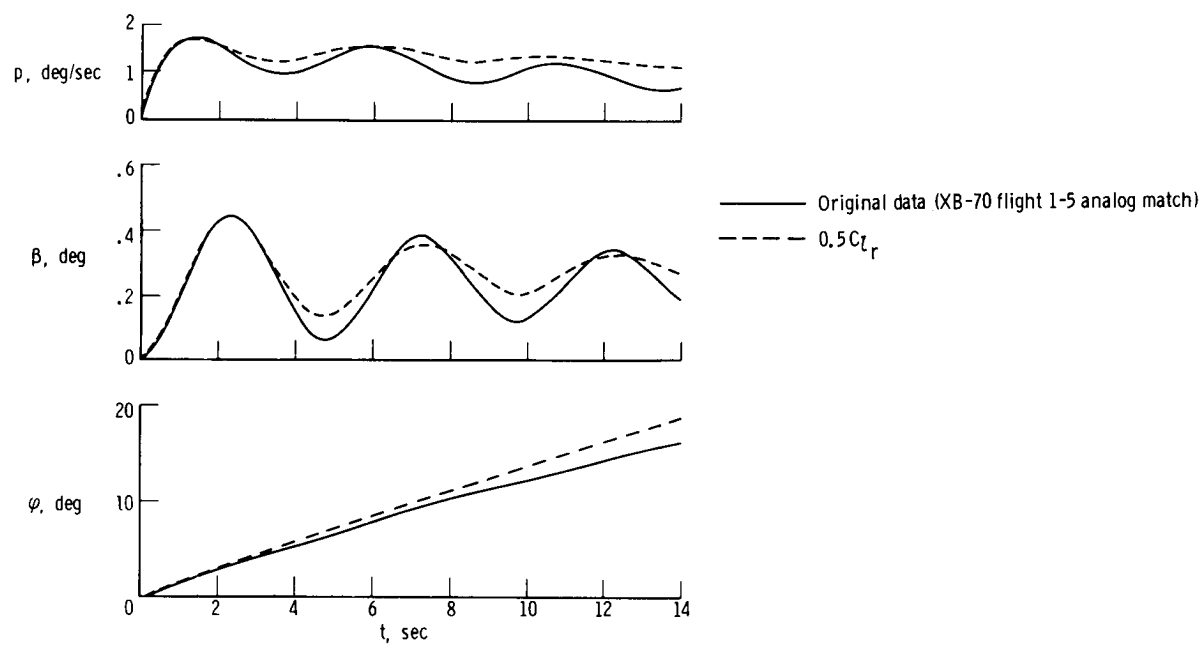

Figure 16. Response of airborne analog computer to 2° δ_a step. Mach 1.2 simulation.

Adverse yaw due to aileron. – The generation of adverse yaw with aileron on the GPAS was considered to be close to that of the XB-70. Approximately 1/2° to 3/4° of sideslip was generated in slow aileron rolls and 1° to 1 1/2° in faster-than-normal rolls. One significant item was noted which illustrated that the simulator had to be flown like the actual vehicle if valid pilot comparisons were to be made. Pilot A commented initially that the GPAS had more yaw due to aileron than the XB-70. He recognized, however, that he was performing aileron rolls in the GPAS at rates (12 to 15 deg/sec) not normally used in the XB-70 at supersonic speeds. When he performed double aileron pulses and turn entries in the GPAS in the same manner as he had in the XB-70, he saw sideslip excursions similar to those he had observed in the XB-70.

Spiral mode. – The pilot was able to distinguish between the 26-second time constant associated with the original GPAS configuration and the 45-second time constant resulting from the 50-percent reduction in C_{l_r}. The latter condition was still

considered to be slightly more convergent than the XB-70 spiral mode but generally representative.

Roll power and roll damping. – The GPAS simulation of XB-70 roll power and roll damping was judged to be good by the pilot; he assigned an SPR of 2. The slight difference in steady-state roll rate between the two configurations (fig. 16) was not noticeable enough to alter his opinion of the roll-mode representation.

Rudder control power. – The pilot commented that rudder control power on the GPAS seemed to be lower than on the XB-70 during the rudder doublets; thus, $C_{n_{\delta_r}}$ was increased 50 percent. The pilot repeated the rudder doublets several times and concluded that, although some improvement was evident, neither the original nor the improved rudder control power settings were very different from those on the XB-70. Apparent low rudder control power on the GPAS was mentioned by other XB-70 pilots and was later attributed to low bandwidth characteristics of the GPAS feel system which made the rudder control system feel sluggish, especially for sharp pilot inputs.

Overall lateral-directional simulation. – The pilot was generally pleased with the simulation after the aileron gradient and Dutch roll damping changes were made. He commented that the original simulation was not representative of the XB-70 (SPR = 5), but termed the final configuration "pretty good" and gave it an SPR of 2.

Simulation of Longitudinal Characteristics

The pilot evaluated the longitudinal dynamics of the simulator for approximately 30 minutes during GPAS flight 45. Unfortunately, he had been exposed to three different longitudinal conditions during XB-70 flight 1-63 and believed he would be unable to compare the GPAS simulation with the XB-70 at one specific condition. However, he did perform several longitudinal maneuvers in the GPAS; some of these are compared with XB-70 responses in the next section.

Pilot A stated that the GPAS was generally representative of the XB-70 in mild longitudinal maneuvers such as climbs and descents of 610 meters (2000 feet). He also commented that the speed response to the throttle was perhaps 50 percent low in the GPAS.

ANALYSIS OF XB-70 FLIGHT 1-63 AND COMPARISON WITH RESULTS OF GPAS FLIGHT 45

Longitudinal

Although the pilot did not make a detailed longitudinal comparison of the XB-70 and the GPAS, he did perform mild maneuvers in the GPAS as he did in the XB-70. Figure 17 shows the analog computer response of a pullup and release maneuver performed on GPAS flight 45 and data from the maneuver performed on XB-70 flight 1-63. Although the inputs are not identical, the similarity in response is evident. The actual JetStar response is shown in figure 18. The acceleration levels at the pilot's location in the GPAS are fairly close to the computed normal acceleration

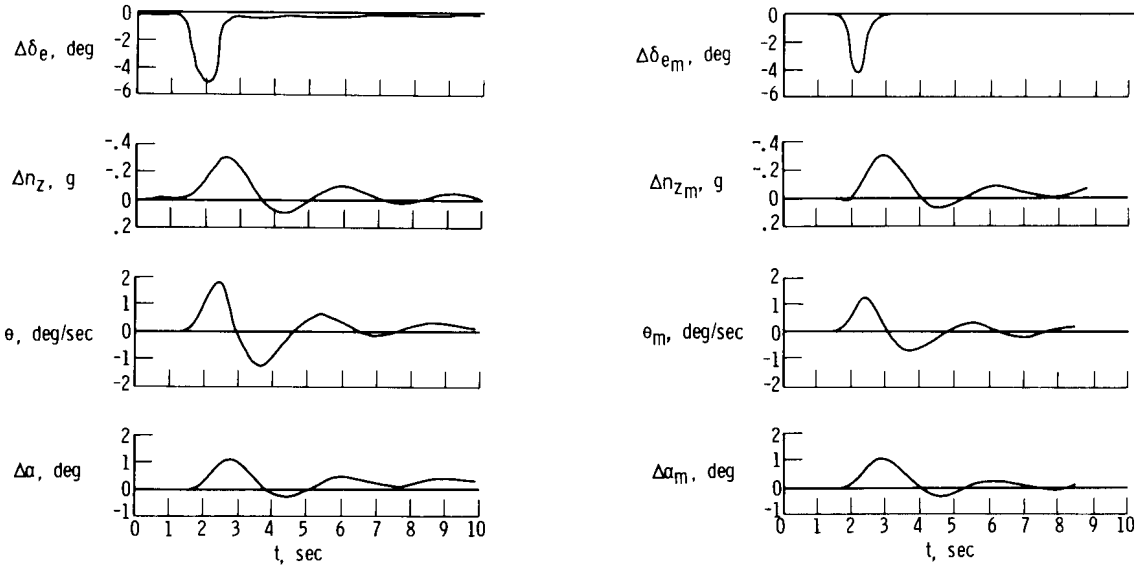

(a) XB-70 flight 1-63. *(b) GPAS flight 45 (analog computer).*

Figure 17. Comparison of pullup and release maneuver on XB-70 and GPAS. Mach 1.2 simulation.

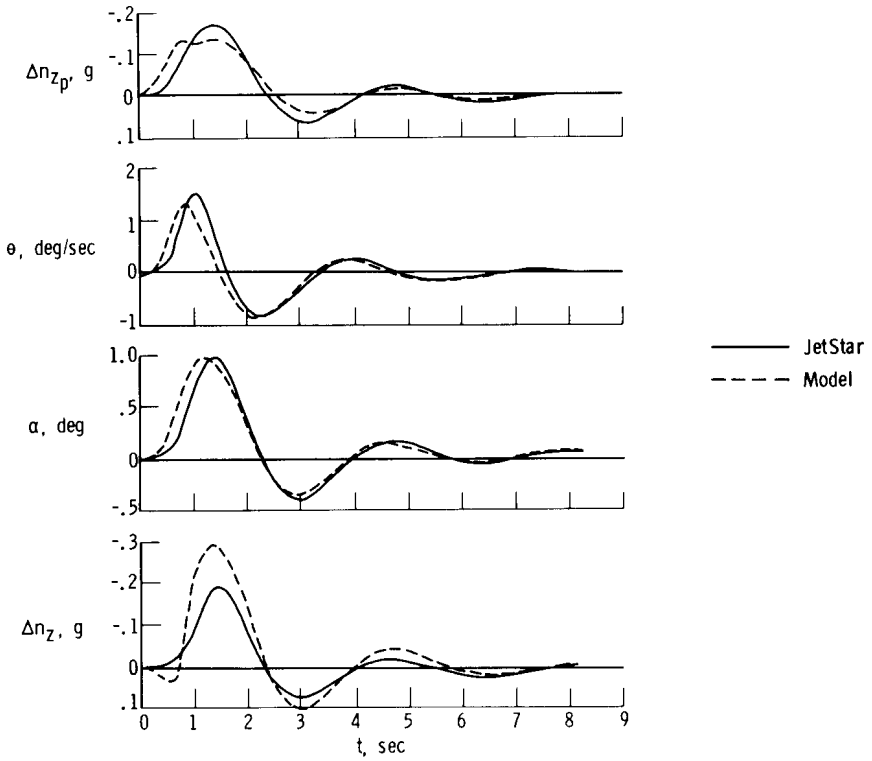

Figure 18. Model-following for a pullup and release maneuver for GPAS flight 45. Mach 1.2 simulation.

at the pilots' location in the XB-70. The angle-of-attack and pitch-rate matches are also good during the short-period oscillation. Angle of attack is matched on a 1:1 basis; thus, the normal accelerations at the airplane's center of gravity differ during the free oscillation because of true speed and lift-curve-slope differences between the simulated XB-70 and actual JetStar flight conditions.

Table 5 compares the longitudinal characteristics programed on the airborne computer with measured XB-70 and JetStar responses. The GPAS short-period frequency and damping agree well with those of the XB-70. The most significant discrepancy is in $\frac{F_e}{n_z}$, in which the GPAS was more than 35 percent too high.

TABLE 5. – COMPARISON OF LONGITUDINAL CHARACTERISTICS OF XB-70 AND GPAS FOR MACH 1.2 SIMULATION

	Measured on XB-70 (flight 1-63)	Programed on GPAS (computer)	Measured on GPAS (flight 45)
ω_{sp}, rad/sec	1.96	2.00	1.97
ζ_{sp}	0.28	0.30	0.29
T_p, sec	Not measured	181	Not measured
ζ_p	Not measured	-0.03	Not measured
n_{z_α}, g/deg	18.0	21.8	15.0
$\frac{F_e}{n_z}$, N/g (lb/g)	472 (106)	400 (90)	645 (145)

Figure 19 compares data from a constant-altitude, full-throttle acceleration during XB-70 flight 1-57 at Mach 1.35 and one during GPAS flight 45. On the basis of

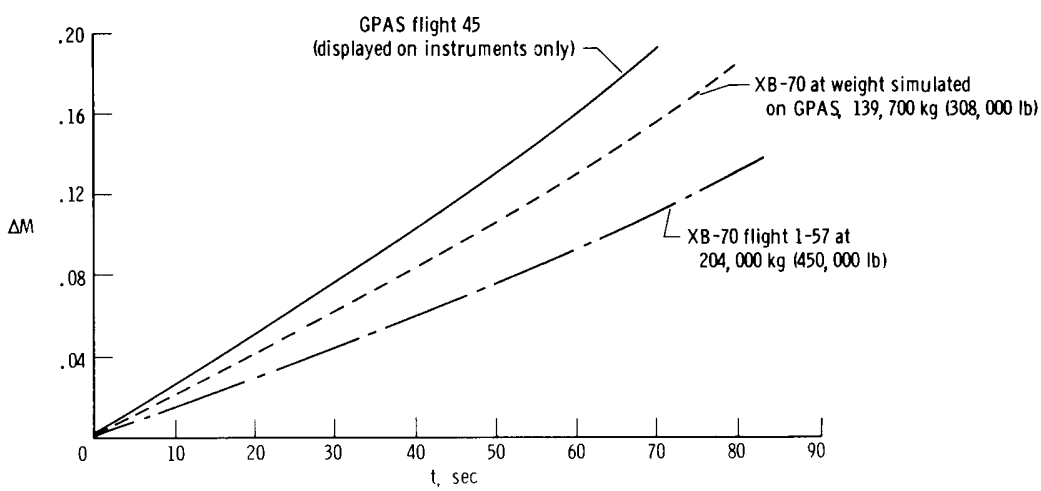

Figure 19. Comparison of constant-altitude acceleration (full throttle) maneuver on XB-70 and GPAS.

the data, the pilot's impression of slow speed response to the throttle in the GPAS does not seem to be justified. Further questioning of the pilot revealed that longitudinal accelerations, n_x, were noticeable in the XB-70 during such a maneuver. The longitudinal-velocity changes were not matched by the JetStar, although these changes were displayed to the pilot on his instruments. A possible cause of the apparent discrepancy is the lack of actual longitudinal acceleration or increased engine noise during thrust changes, although no attempt was made to demonstrate this.

It can be assumed, then, that items such as those shown in table 5 can be duplicated accurately. How well the JetStar could match the more subtle items (yet important to the pilot) such as speed stability is not known. This information was considered to be of secondary importance in the GPAS validation program, because factors such as trim characteristics are more nearly a pure function of input data accuracy and the instrument display than of motion and visual effects of concern in an airborne simulator.

Lateral-Directional

Time histories of rudder and aileron doublets from XB-70 flight 1-63 were analyzed and analog-matched after the GPAS validation flight. The resulting stability derivatives and modes were then compared with those for the final configuration reached on GPAS flight 45 primarily to determine why changes were necessary to the airborne computer to satisfy the pilot that the XB-70 characteristics were being simulated.

Model-following during flight 45 was found to be good, with the exception of n_{y_p} matching. Figure 20 is a typical example of the quality of reproduction of computer-commanded motions. The actual measurements of JetStar responses shown in the

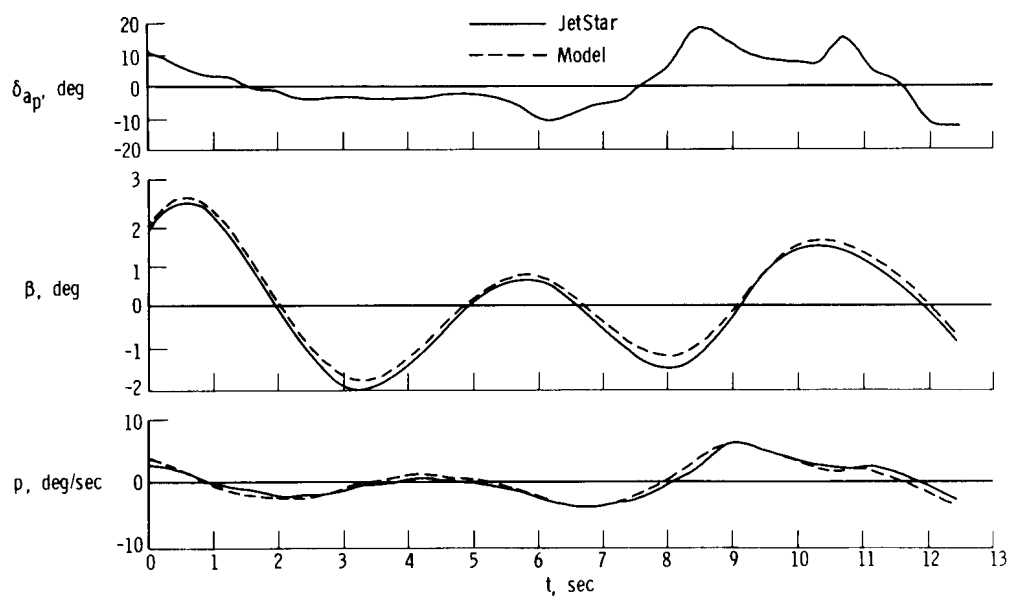

Figure 20. Model-following on GPAS flight 45. Mach 1.2 simulation.

figure confirm that the lateral-directional dynamic characteristics of the computer model had been duplicated well by the JetStar. Lateral acceleration at the pilot's location is discussed in reference 5.

The static characteristics of the XB-70 and final GPAS configuration are compared in figure 21. The δ_r versus β and δ_a versus β data agree fairly well, but the F_{r_p} versus β and F_{a_p} versus β data reflect the feel system static mismatch that is known quantitatively from figure 14 for the aileron feel and from figure 15 for the rudder feel.

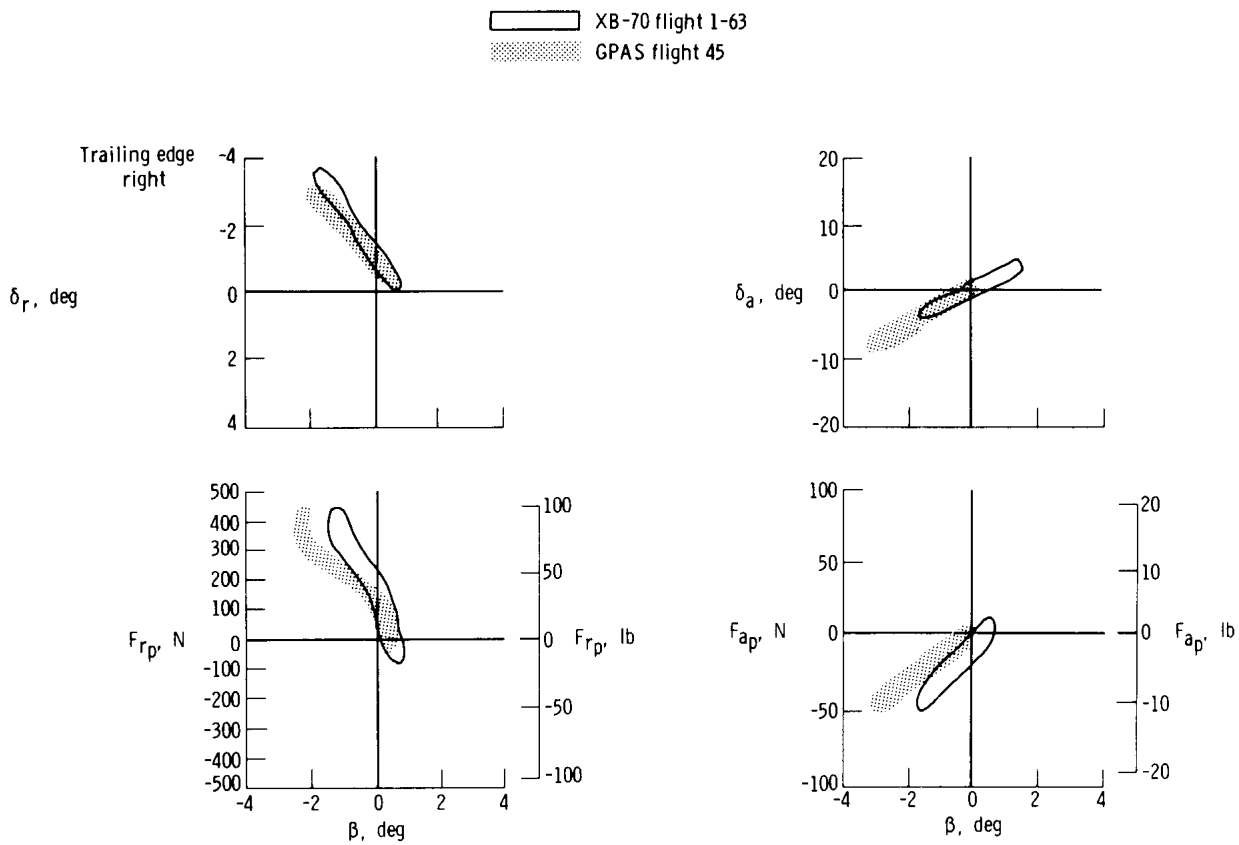

Figure 21. Comparison of XB-70 and GPAS static characteristics in a wings-level sideslip. Mach 1.2 simulation.

As expected, the XB-70 did not fly at the same weight and center of gravity as the condition programed on the GPAS. The flight conditions are compared in the following table:

Parameter	GPAS flight 45 simulated condition	XB-70 flight 1-63 actual condition
Mach number	1.20	1.21
Altitude, m (ft)	12,600 (41,500)	12,000 (39,500)
Gross weight, kg (lb)	139,700 (308,000)	175,000 (386,000)
Center of gravity, percent mean aerodynamic chord	21.65	19.85
Dynamic pressure, N/m^2 (lb/ft^2)	17,700 (370)	19,700 (411)

The weight and center-of-gravity difference is significant for the XB-70. As mentioned previously, in-flight changes required in the basic GPAS simulation could be attributed, in part, to a mismatch of flight conditions between the condition programed and the condition flown in the actual vehicle for validation purposes.

Comparison of Stability Derivatives and Dynamic Characteristics

The stability derivatives obtained from analog-matching a well-conditioned aileron and rudder doublet from XB-70 flight 1-63 are shown in table 6 with the original derivatives (from flight 1-5) and the original data corrected to the same weight and

TABLE 6. – COMPARISON OF STABILITY DERIVATIVES OBTAINED FROM XB-70 ANALOG MATCHING

Stability derivative, rad^{-1}	Original data (flight 1-5) for XB-70	Original data (flight 1-5) corrected to flight 1-63 weight and center of gravity	Flight 1-63 match data
$C_{Y_{\delta_a}}$	0.00264	0.00108	0.007151
$C_{Y_{\delta_r}}$	.11231	.1113	.1182
C_{Y_β}	.3883	-.3886	-.3540
$C_{l_{\delta_a}}$	-.00991	.00972	.00975
$C_{l_{\delta_r}}$	-.01232	-.0123	.0018
C_{l_r}	-.3662	-.3617	-.09058
C_{l_β}	-.01266	-.0246	-.03329
C_{l_p}	-.2250	-.2184	-.1975
$C_{n_{\delta_a}}$	-.00246	.000464	-.00829
$C_{n_{\delta_r}}$	-.06389	-.0644	-.0613
C_{n_r}	-.4666	-.4690	-.1173
C_{n_β}	.09856	.1059	.1076
C_{n_p}	-.18590	-.1830	.02695

center-of-gravity condition as that of flight 1-63. As shown, although a lower absolute value of C_{l_r} was obtained from the second analog match, as was required on GPAS flight 45, several other stability derivatives changed significantly. To compare the GPAS results with the analog-matched data, several modal parameters for a number of conditions of interest are listed in table 7.

TABLE 7. – COMPARISON OF DYNAMICS OF SEVERAL PERTINENT CONFIGURATIONS RELATED TO XB-70 AT MACH 1.2

Parameter	Original flight 1-5 data	Flight 1-5 data corrected to flight 1-63 weight and center of gravity	Flight 1-63 match data	GPAS flight 45 (measured)	Measured XB-70 characteristics
ω_ψ, rad/sec	1.29	1.24	1.21	1.30	1.23
ζ_ψ	.056	.050	.138	.11	.11
τ_r, sec	.56	.71	.99	.40	Not measured
τ_s, sec	25.9	23.9	65.2	50.0	Not measured
$\left\lvert\frac{\varphi}{\beta}(s)\right\rvert_\psi$	1.45	2.20	2.59	1.05	2.90
Angle $\frac{\varphi}{\beta}(s)_\psi$, deg	1.50	16.9	29.2	10.0	20.0
$\frac{\omega_\varphi}{\omega_\psi}$	.89	.84	.71	Not measured	Not measured
p_{ss}, deg/sec/deg	.74	.68	.71	.66	Not measured

From the table it can be concluded that:

(1) The Dutch roll damping ratio $\zeta_\psi = 0.056$ of the original (flight 1-5 data) configuration was too low, as detected by pilot A.

(2) The correction of the flight 1-5 data to the flight 1-63 weight and center-of-gravity condition did not bring ζ_ψ closer to that measured on the XB-70.

(3) The final GPAS Dutch roll damping which pilot A stated was close to that of the XB-70 ($\zeta_\psi = 0.11$) is close to measured and calculated values for the XB-70, based on flight 1-63 data.

(4) The analog match of XB-70 flight 1-63 shows a more neutral spiral mode than the original data. This corresponds to pilot comments made during GPAS flight 45 that the original spiral-mode representation ($\tau_s = 25.9$ sec) was too strongly convergent and that the final GPAS spiral mode ($\tau_s = 50.0$ sec) was more representative of the XB-70.

(5) The actual XB-70 $\left\lvert\frac{\varphi}{\beta}(s)\right\rvert_\psi$ ratio (2.90) is nearly triple the value of the final GPAS value (1.05). The discrepancy in flight condition between the XB-70 as flown by pilot A and as simulated on the GPAS is part of the problem. The flight 1-5 data, when corrected to the 1-63 flight condition, increased the $\left\lvert\frac{\varphi}{\beta}(s)\right\rvert_\psi$ ratio 50 percent. The difference in this ratio was not suspected before GPAS flight 45, and pilot A, who apparently did not notice the discrepancy, made no comment which could stem from this difference.

(6) From the flight 1-63 analog-match data, the XB-70 roll mode time constant τ_r was calculated to be approximately 1 second, which is more than double the resulting GPAS value. The GPAS time constant was measured from the point where the

JetStar roll rate began to respond, approximately 0.2 second after the model began to respond, as shown in figure 22. This dead time is assumed to be similar to XB-70 control-system lags, as mentioned previously. It is not surprising that the pilot apparently did not observe the discrepancy, because both time constants are relatively short.

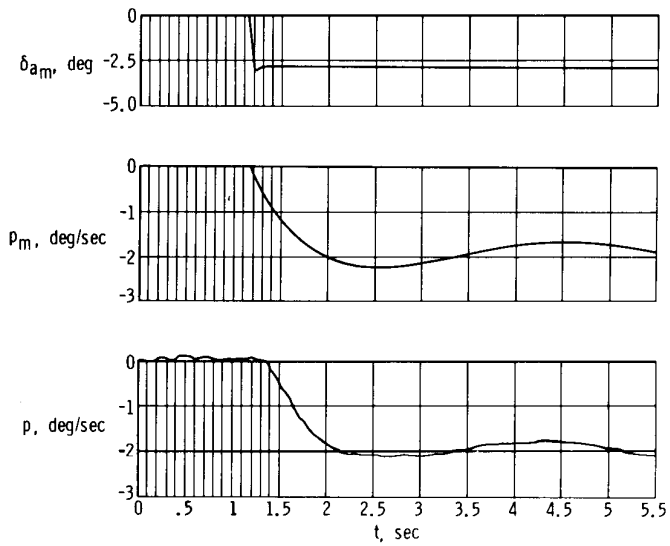

Figure 22. Model and JetStar roll-rate response to δ_{a_m} step on GPAS flight 45. Original configuration; Mach 1.2 simulation.

Table 8 lists the programed and the measured characteristics for the airborne computer and the GPAS response, respectively. The two agree favorably. The computed $\frac{\omega_\varphi}{\omega_\psi}$ ratio for the programed configuration (0.89) is significantly higher than the value computed from the flight 1-63 derivatives.

TABLE 8. – COMPARISON OF PROGRAMED AND MEASURED CHARACTERISTICS OF GPAS FLIGHT 45 FINAL RESULTS

Parameter	Programed on airborne analog computer	Measured JetStar response
ω_ψ, rad/sec	1.29	1.30
ζ_ψ	.107	.11
τ_r, sec	.58	.4*
τ_s, sec	45.3	50
$\left\lvert \frac{\varphi}{\beta}(s) \right\rvert_\psi$	1.14	1.05
Angle $\frac{\varphi}{\beta}(s)_\psi$, deg	18.3	10.0
$\frac{\omega_\varphi}{\omega_\psi}$	.89	Not measured
p_{ss}, deg/sec/deg	.77	.66

*Does not include apparent transport delay of 0.2 second.

Further Time-History Comparisons

To verify that the derivatives obtained from the second analog match of XB-70 flight 1-63 represented the XB-70 accurately, a direct time history correlation was made by the method shown in the flow chart of figure 23. The rudder-pedal position during a double rudder pulse from flight 1-63 was recorded on FM tape. During a GPAS flight, the tape was played back directly into the analog computer as a pilot command.

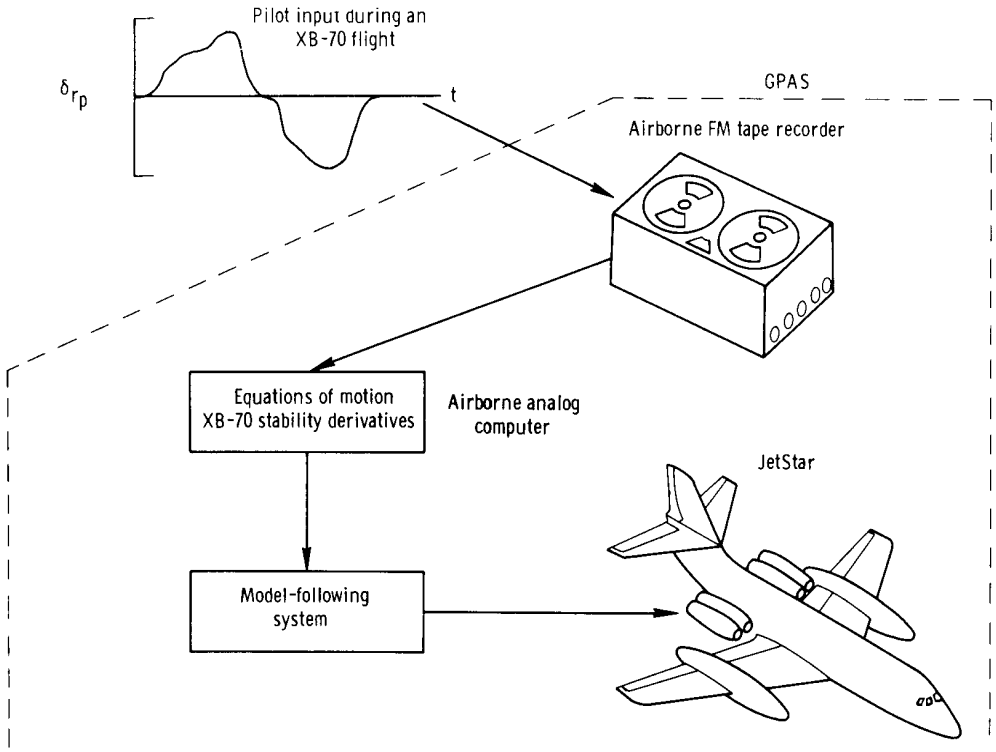

Figure 23. Method of obtaining in-flight response comparisons between GPAS and XB-70.

The computer was programed with the new (flight 1-63) derivatives. The JetStar response to this input was then compared with the actual XB-70 response, as shown in figure 24. The solid line is the actual XB-70 response plotted directly from the XB-70 data-recording system. The open circles are points read from the GPAS recording system which were superimposed on the XB-70 time history. The JetStar response is remarkably close to that of the XB-70; the roll-rate responses are nearly coincident. Thus, the lag due to model-following in the GPAS is that required to duplicate the control-system lags in XB-70, as had been assumed earlier.

Figure 20 showed that sideslip-following in the GPAS is accomplished with almost no phase lag. In figure 24 it is clear that the GPAS leads the XB-70 in sideslip by approximately 0.2 second to 0.3 second. Thus, it would be expected that the $\frac{\varphi}{\beta}(s)$ phase angle for the JetStar would be slightly less (10°) than that of the XB-70 (20°). Figure 24 indicates that the derivatives obtained from the analog match of flight 1-63

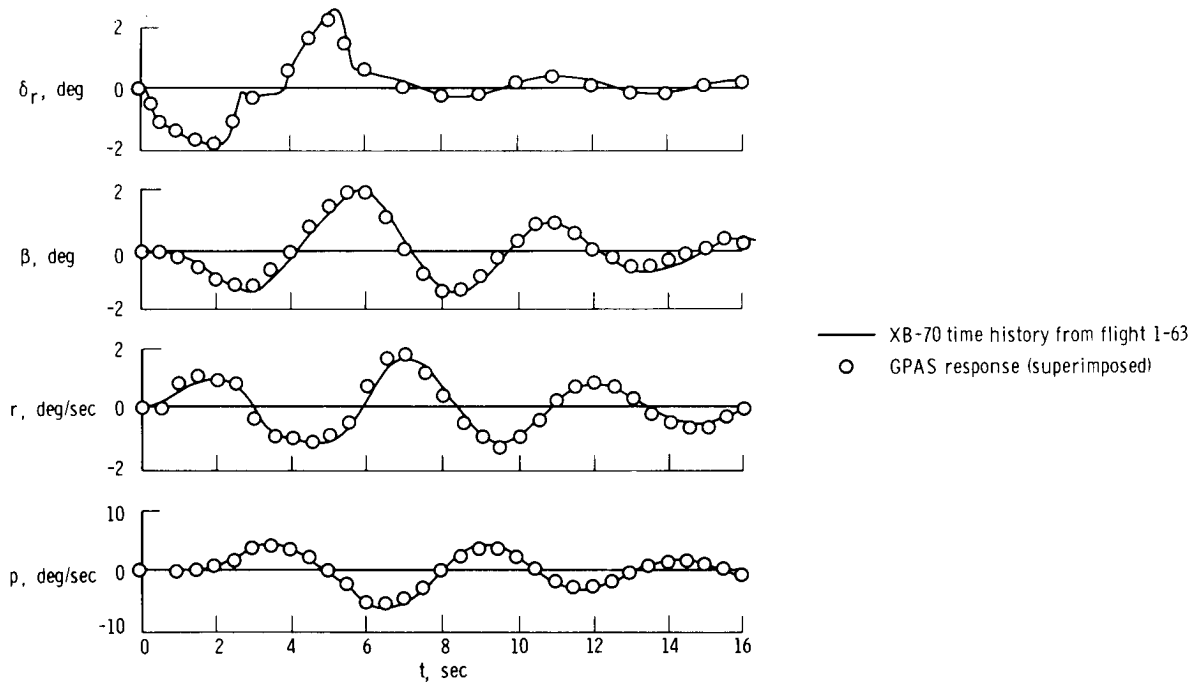

Figure 24. GPAS match of XB-70 maneuver. Mach 1.2 simulation.

represent the XB-70 well when programed on the GPAS and when model-following is of good quality. It is also apparent that the model-following lags of 0.2 second to 0.4 second commonly observed in the GPAS resulted in a JetStar response which closely matched that of the actual XB-70 response. It should be noted, however, that this may not necessarily be the situation for any particular vehicle to be simulated. It would be more desirable to match response variables with nearly zero lag and then mechanize the actual (or desired) control system dynamics on the airborne computer.

Conclusions on the Validation With the XB-70 at Mach 1.2

A configuration was obtained on GPAS flight 45 which was judged by the evaluation pilot to be a good simulation of the XB-70 at Mach 1.2. Table 7 shows that this GPAS configuration was close to the actual XB-70 with respect to Dutch roll damping, but that it differed slightly with respect to $\left|\frac{\varphi}{\beta}(s)\right|_{\psi}$, τ_r, and $\frac{\omega_\varphi}{\omega_\psi}$. Although the $\left|\frac{\varphi}{\beta}(s)\right|_{\psi}$ ratios differed by a large percentage, both values are small and the difference was not noticed by the pilot. The difference may not be distinguishable for these particular Dutch roll dynamics. A similar argument can be used for the roll-mode time constants $\tau_{r_J} = 0.4$ and $\tau_{r_{XB-70}} = 0.99$, because aileron control is normally applied in a mild manner for the XB-70 and for the GPAS flown like the XB-70. It should be recognized that if discrepancies in certain items are below pilot threshold sensitivity levels, there is little possibility that the pilot will note any gross differences.

The discrepancy in the calculated $\frac{\omega_\varphi}{\omega_\psi}$ ratio for XB-70 flight 1-63 data and the

final GPAS configuration must be considered carefully, because proper simulation of this quantity is necessary if a simulator is to be useful in general handling-qualities research. Examination of model-following in p and β leads to the conclusion that the $\frac{\omega_\varphi}{\omega_\psi}$ ratio the pilot saw in the final GPAS configuration was essentially that programed on the model $\frac{\omega_\varphi}{\omega_\psi} = 0.89$. This configuration has a roll response which is not too greatly contaminated with Dutch roll, as shown in figure 16. The pilot's comments were as expected for this fairly high $\frac{\omega_\varphi}{\omega_\psi}$ value. He thought that the roll response was generally smooth, with little "stepping" action due to Dutch roll excitation, and that this roll mode representation matched what he observed in the XB-70.

The final XB-70 matched derivatives yielded a calculated $\frac{\omega_\varphi}{\omega_\psi}$ value of 0.71; however, the resulting roll response was heavily contaminated with Dutch roll. An analog computer time history of an aileron step to this set of derivatives is shown in figure 25.

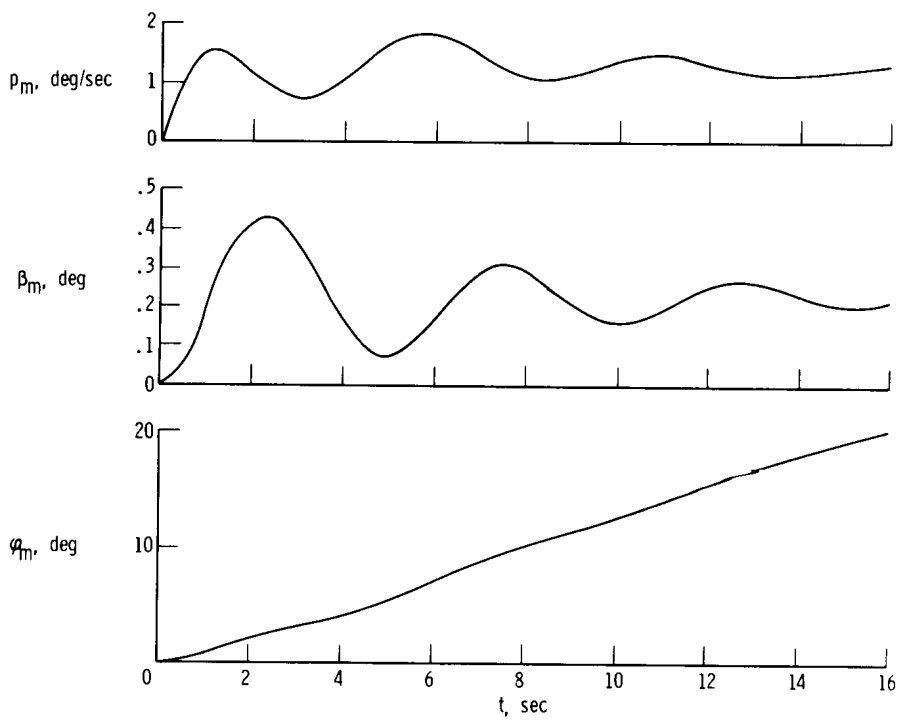

Figure 25. Response of analog computer to 2° aileron step at t = 0 sec. Analog-match data from XB-70 flight 1-63; Mach 1.2 simulation.

In previous GPAS flights, the pilots, including pilot A, were aware of the oscillatory roll response for $\frac{\omega_\varphi}{\omega_\psi} < 0.75$. Pilot A stated, however, that the XB-70 had a smooth, unhesitating roll response. It is apparent that the GPAS was not distorting the $\frac{\omega_\varphi}{\omega_\psi}$ ratio that was programed, because the GPAS response is precisely that expected for

this $\frac{\omega_\varphi}{\omega_\psi}$ value. Therefore, it must be concluded that either the XB-70 did not have an $\frac{\omega_\varphi}{\omega_\psi}$ value of 0.71, indicating uncertainties in the derivatives, or the pilot's impression of the XB-70 roll response was distorted either by the XB-70 field of view or attitude instrument display. It would have been beneficial, of course, to have pilot A evaluate the final set of derivatives on the GPAS, but operational and scheduling considerations prevented this.

The most significant results of the validation with the XB-70 at Mach 1.2 were as follows:

(1) The time lapse between actual aircraft evaluation and simulator evaluation should be the shortest possible. Although pilot A could make only gross assessments of the GPAS fidelity on his orientation flight (several weeks after an XB-70 flight), he was able to make positive statements about the XB-70 simulation during the GPAS validation flight (3 days after an XB-70 flight at the same flight condition simulated). He believed this 3-day period was as long as would be desired.

(2) The pilot selected aileron wheel force and Dutch roll damping as the most significant discrepancies in the GPAS simulation of the XB-70. He also believed that the GPAS spiral mode was too strongly convergent.

(3) A 30-percent decrease in aileron force gradient from the measured XB-70 values satisfied pilot A that the aileron feel was properly represented.

(4) A 50-percent decrease in the stability derivative C_{l_r} increased Dutch roll damping and weakened the spiral convergence so that the pilot termed the overall lateral-directional simulation "good."

(5) While performing aileron rolls in the GPAS at higher rates than normally commanded in the XB-70, the pilot had the impression that adverse-yaw generation was too high, but, while maneuvering the GPAS in the manner he flew the XB-70, he believed adverse yaw was similar to that experienced in the XB-70.

(6) The aerodynamic stability derivatives obtained from analog-matching maneuvers from XB-70 flight 1-63 resulted in a configuration only slightly different from the final GPAS configuration, which pilot A rated "good." The major difference was in the calculated value of $\frac{\omega_\varphi}{\omega_\psi}$. This discrepancy was not resolved. The GPAS flight records showed good fidelity in reproducing programed characteristics. The pilot's failure to observe the small differences which apparently existed between the XB-70 and GPAS, in light of the generally high quality of mode simulation, leads to the conclusion that the discrepancies were within the pilot's threshold of observability.

GPAS SIMULATION OF XB-70 AT MACH 2.35

At Mach 2.35 and 16,800 meters (55,000 feet) altitude the XB-70 exhibited adverse yaw due to aileron but had negative dihedral, in contrast with the Mach 1.2 at 12,200 meters (40,000 feet) altitude condition. At this condition, the aircraft, without stability augmentation, had a PIO tendency, but the Dutch roll was positively damped, hands off. Because simulation fidelity would probably be critical in properly representing the PIO condition, it was thought that this condition would tax the GPAS simulation capability more than the Mach 1.2 at 12,200 meters (40,000 feet) altitude dynamics.

XB-70 FLIGHT 1-68

On October 11, 1967, the XB-70 was flown by pilot B for approximately 30 minutes at Mach 2.35 (flight 1-68). The pilot had approximately 20 minutes of evaluation time at Mach 2.35 during the flight. A detailed pilot questionnaire was written and discussed with pilot B prior to the flight. A portion of the questionnaire is presented in appendix D. A GPAS flight (53) was made before XB-70 flight 1-68 to allow pilot B to practice the standard set of stability and control maneuvers as well as special rolling maneuvers involving small and precise bank-angle changes. The pilot was able to complete all planned maneuvers at this flight condition on XB-70 flight 1-68. His report for this portion of the flight and additional comments made during a postflight debriefing are presented in appendix E. He believed that the XB-70 differed in two ways from the GPAS simulation: (1) The XB-70 was more difficult to fly than the GPAS, and (2) the Dutch roll in the XB-70 appeared to be primarily a yaw oscillation, whereas the GPAS had much roll oscillation along with the yaw motion. Telemetry data from the XB-70 flight did not reveal any obvious discrepancies between the XB-70 and the dynamics programed on the GPAS.

PRIMARY GPAS VALIDATION FLIGHT (54)

On October 12, 1967, pilot B flew the GPAS simulation of the XB-70 for more than 3 hours. The flight plan (appendix F) required him to repeat all maneuvers performed on the XB-70 the previous day in the manner they were performed on the XB-70.

Simulation of Feel-System Characteristics

Elevator. – The pilot considered the elevator feel to be a good simulation of that of the XB-70 and assigned an SPR of 2. GPAS and XB-70 elevator feel-system control cycles are compared in figure 26.

Aileron. – The original and best known XB-70 aileron feel-system characteristics were set up on the GPAS. Pilot B considered the simulation to be good, except near the center position where the GPAS forces seemed to be too high. He stated that in

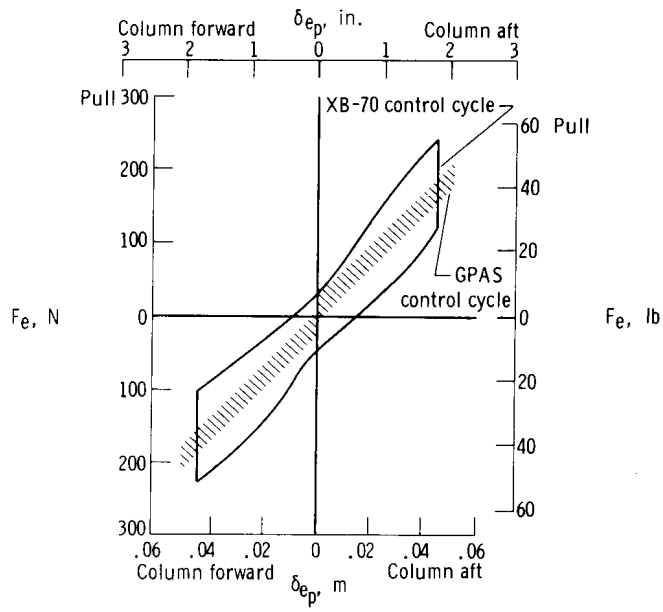

Figure 26. Comparison of static characteristics of GPAS and XB-70 elevator feel systems. Mach 2.35 simulation.

the ±5° range the XB-70 gradient felt more shallow than the simulated gradient and asked that the 8.9-newton (2.0-pound) breakout force programed in the GPAS be removed. He was satisfied with this change and assigned an SPR of 2. Control cycles of the XB-70 and GPAS aileron feel systems are compared in figure 27.

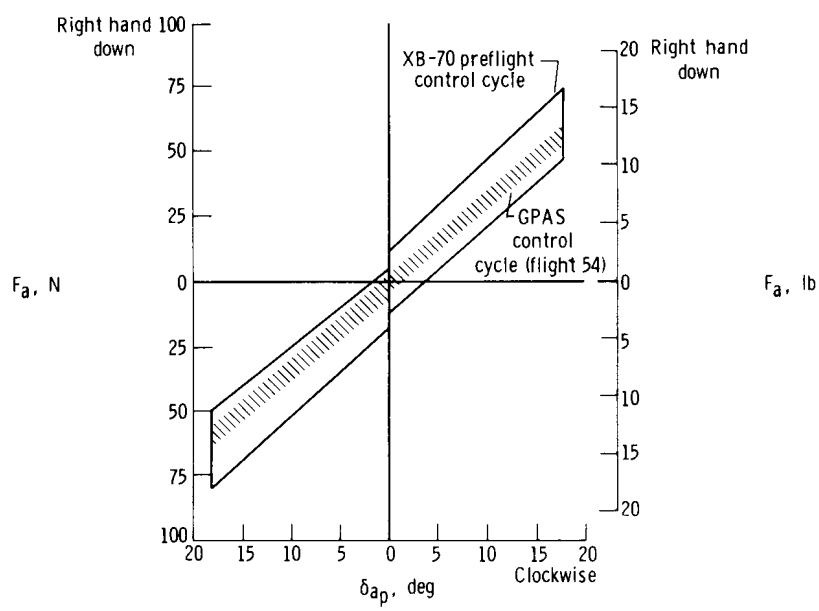

Figure 27. Comparison of static characteristics of XB-70 and final GPAS aileron feel systems for GPAS flight 54. Mach 2.35 simulation.

Rudder. – An SPR of 2 was given the rudder feel system, with no significant discrepancies noted. Static characteristics of the XB-70 and GPAS rudder-feel systems

are compared in figure 28.

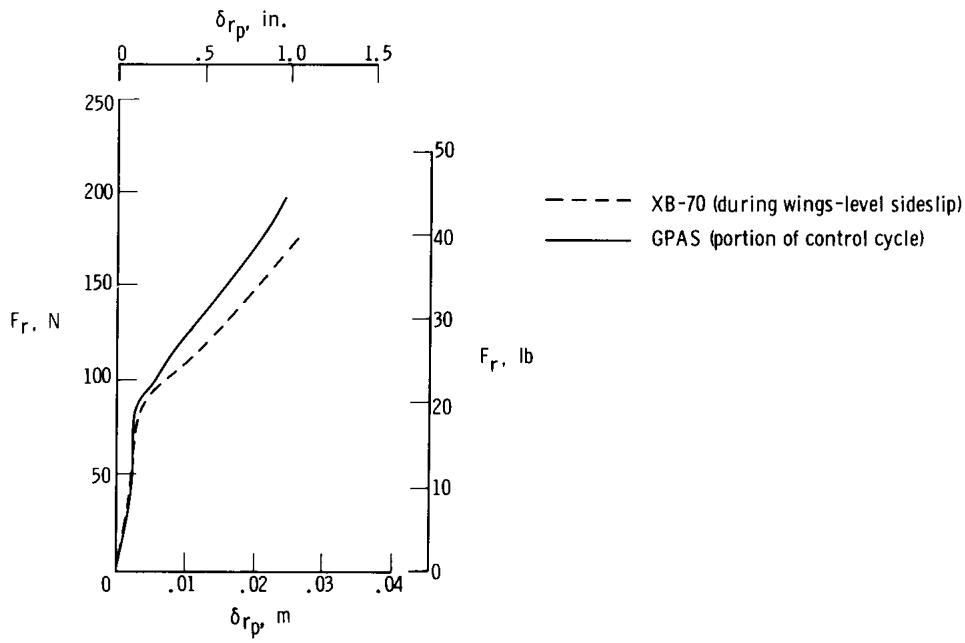

Figure 28. Comparison of static characteristics of XB-70 and GPAS rudder feel systems. Mach 2.35 simulation.

Simulation of Lateral-Directional Characteristics

The pilot commented that the major discrepancies in the basic GPAS simulation of the Mach 2.35 condition were that the GPAS did not present as difficult a PIO problem as the XB-70 and appeared to have a higher roll component in the Dutch roll. An additional comment concerning high GPAS Dutch roll damping was the key to the PIO discrepancy.

Three aerodynamic stability derivatives were changed during the flight to provide what the pilot considered to be a good simulation. The changes were: (1) C_{l_β} was reduced 25 percent; (2) C_{n_r} was reduced 43 percent; and (3) $C_{n_{\delta_a}}$ was increased 50 percent. The change in C_{n_r} was made in several steps, with the pilot making a short evaluation of damping and PIO after each change and then directing an appropriate change. Table 9 summarizes pilot comments on the changes made during the flight in the order in which the changes were made. Table 10 is a compilation of simulation pilot ratings for the original and final configurations. The wings-level sideslip maneuver proved to be excellent for the validation task, because it contained directional disturbances (through rudder) and a tight bank-angle tracking task (maintain $\varphi = 0^\circ$). This maneuver was ideal for testing the PIO tendencies of the GPAS simulation.

Roll-to-yaw ratio. – The pilot considered the GPAS roll-to-yaw ratio to be different from that of the XB-70 both in a free oscillation and during the wings-level sideslip

TABLE 9. – PILOT B COMMENTS ON GPAS FLIGHT 54 SUMMARY

	PIO tendency	Dutch roll damping	Roll-to-yaw ratio in Dutch roll	Wings-level sideslip	Spiral mode	Roll power	Yaw due to aileron	Overall lateral-directional simulation fidelity
Original configuration	Job is so much easier here; can damp oscillations with aileron. You don't set up a PIO here with small inputs.	GPAS damps out too quickly. The time to damp is about 50 percent less here. The XB-70 seemed to have a residual oscillation.	Too much rolling in the Dutch roll. XB-70 appeared to oscillate primarily in yaw. There is considerably more rolling here.	Similar yaw angle and wheel required as in the XB-70. My inputs are different here. There is more rolling here, and that requires more inputs.	The XB-70 rolled off one direction or another. The GPAS rolls off slightly.	Roll power itself is representative of the XB-70, but you don't use much at high speed.	It seems like I got a little more sideslip for small wheel deflections in the XB-70, but the GPAS is pretty close.	Overall the SPR is a 3+. It is not unrepresentative. I would say damping and rolling in the Dutch roll are farthest off.
$0.75C_{l_\beta}$	PIO less than first case. This is easier to fly. We have moved away from the XB-70 in this respect.	I don't see much difference in time to damp. The damping needs to come down.	It certainly appears that you have cut down the roll motion in the Dutch roll. The XB-70 might still have a little less rolling.	There seems to be an overall reduction in rolling during Dutch roll oscillations.	No comments.	Aileron effectiveness seems to be less here.	No change.	Not as good as first configuration. Easier to fly, less PIO. This case is closer only with respect to rolling.
$0.57C_{n_r}$ $0.75C_{l_\beta}$	When you are in the loop. The PIO is very close to the XB-70, but it is not as easy here to initiate a PIO.	Damping close to XB-70. You have got the directional looseness just about like the XB-70.	Pretty close to XB-70. XB-70 may not roll quite this much, but you're not far off.	Workload on the same order as in XB-70. Sideslip and wheel angles close to XB-70 for full rudder.	No comments.	Roll power seems to be very good and representative of the XB-70.	I generate pretty much the same yaw here, although I think small wheel inputs give you a little more yaw in XB-70.	This looks good. SPR = 2 1/2. Looks like the XB-70 for pulses, sideslips, and PIO. Only big difference is the onset of PIO.
$1.5C_{n_{\delta_a}}$ $0.57C_{n_r}$ $0.75C_{l_\beta}$	In this configuration I find I have to be careful or else I get sideslip increasing, which is exactly like I found in the XB-70.	The only thing is that the GPAS will damp out completely hands off, and I never did see that in the XB-70 yesterday.	You are very close to the XB-70.	Pretty close to XB-70. I use 9° to 10° of wheel and get about 1 1/2° of sideslip. Workload about the same as on XB-70.	This doesn't tend to roll off like the XB-70 did. If I let go on the XB-70, it would roll off one way or the other.	I don't see anything different here.	I see the same ±1/2° to ±3/4° for this type of wheel motion. Yaw generation close to that of XB-70.	This configuration is a good simulation of the XB-70. SPR = 2. The only real difference is that the XB-70 never did damp completely.

TABLE 10. – SIMULATION PILOT RATINGS ASSIGNED TO GPAS SIMULATION (FLIGHT 54) OF XB-70 AT MACH 2.35

	Simulation pilot rating
Basic configuration:	
Elevator feel system	2
Aileron feel system	2
Rudder feel system	2
Aileron centering	2
Wings-level sideslip (task)	3.5
Roll-to-yaw ratio	3
Roll off with rudder	2.5
Dutch roll damping	4
Lateral-directional maneuver	3
Overall lateral-directional	3.5
$0.57\,C_{n_r}$, $0.75\,C_{l_\beta}$:	
Overall lateral-directional	2.5
Dutch roll damping	2
Wings-level sideslip (task)	2
Initiation of PIO	3
Roll-to-yaw ratio	2.5
$0.57\,C_{n_r}$, $0.75\,C_{l_\beta}$, $1.5\,C_{n_{\delta_a}}$:	
Overall lateral-directional	2
Initiation of PIO	2

when more wheel manipulation was required to hold wings level in the GPAS because of more rolling in the Dutch roll oscillations. A 25-percent reduction in C_{l_β}, which reduced the $\left|\frac{\varphi}{\beta}(s)\right|_\psi$ ratio from approximately 2.2 to 1.4, apparently corrected the situation. According to the pilot, this change alone made the total simulation less representative of the XB-70 because the PIO tendency was reduced as well.

PIO tendency and Dutch roll damping. – The PIO tendency and Dutch roll damping are discussed jointly because of the strong influence of ζ_ψ on the PIO situation. Pilot B was certain that the Dutch roll damping for the GPAS was too high. In the process of decreasing the damping ratio on the GPAS, it was apparent that the PIO tendency was being simulated more closely. The pilot performed double aileron pulses and wings-level sideslips to judge Dutch roll damping and the PIO simulation after each change in C_{n_r}. The sequence of changes and brief pilot comments concerning the damping and PIO are shown in table 11. The PIO sensitivity to damping ratio is reflected in the pilot comments for the last four configurations, which had nearly constant values of $\frac{\omega_\varphi}{\omega_\psi}$. The last configuration shown still differed from the XB-70 in the initiation of the PIO, according to the pilot. Once the pilot was coupled into the loop, he thought the situation represented was realistic. However, he stated that once he had damped the oscillation he did not find it as easy to start the PIO again in the GPAS as in the XB-70. For this reason and because he believed the GPAS was slightly low on adverse yaw due to aileron, $C_{n_{\delta_a}}$ was increased 50 percent over its basic value.

TABLE 11. – STABILITY-DERIVATIVE CHANGES AND PILOT COMMENTS ON GPAS FLIGHT 54

Configuration	Dutch roll damping	$\frac{\omega_\varphi}{\omega_\psi}$	Pilot comments on Dutch roll damping	Pilot comments concerning PIO on GPAS
Basic	0.163	1.16	Too high	Not enough
$0.75\,C_{l_\beta}$	.152	1.10	No change	Easier than basic
$0.5\,C_{n_r}$*	.084	1.11	A little low	Little worse than XB-70
$0.65\,C_{n_r}$*	.105	1.11	A little high	Not quite as much as XB-70
$0.57\,C_{n_r}$*	.094	1.11	Pretty close	Close to the XB-70 once pilot is in the loop

*Includes 25-percent reduction in C_{l_β}.

This final GPAS configuration was judged to be a good simulation of the PIO situation in the XB-70, both in initiating it and forcing it once the PIO had developed. The pilot commented, "In this configuration I have to be real careful or I get coupled into the loop and find the sideslip increasing more than I want it to, which is exactly what I found on the XB-70." The pilot assigned a PIO rating (fig. 11) of 3.5 to this configuration, the same as he had rated the XB-70.

The Dutch roll damping was believed to be close to that of the XB-70. The pilot mentioned, however, that the GPAS would damp out completely, hands off, where the XB-70 seemed to have a residual oscillation.

Roll power. – There were no adverse comments concerning roll-power simulation on the GPAS. When C_{l_β} was reduced 25 percent, the pilot noted a decrease in apparent roll power, but believed that the roll power was still representative of the XB-70. (The reduction in C_{l_β} reduced $\left(\frac{\omega_\varphi}{\omega_\psi}\right)^2$ and, hence, the effective roll power.) In addition, the pilot believed that the lag between wheel input and roll response was represented well on the GPAS.

Adverse yaw due to aileron. – The primary complaint regarding adverse yaw due to aileron was that yaw generation seemed smaller on the GPAS for small (±2 to 4°) wheel inputs. Increasing $C_{n_{\delta_a}}$ by 50 percent corrected the discrepancy and improved the simulation of PIO initiation, as previously mentioned.

Spiral mode. – The pilot stated several times that in the spiral mode the XB-70 had a noticeable tendency to roll off in either direction. This required frequent wheel inputs which tended to initiate a PIO. The original configuration evidently showed some of this rolloff characteristic (table 9), but the final configuration did not.

Rudder power. – No strong comments were made concerning the rudder power, primarily because rudder was not used much during the flight. The pilot did mention that in the GPAS sharp rudder inputs did not seem to be as effective in damping the Dutch roll oscillations as in the XB-70. These comments are consistent with others concerning low rudder power or high rudder forces and most likely result from feel

system frequency-response limitations.

Overall lateral-directional simulation. – Pilot B was generally well pleased with the final lateral-directional simulation. He assigned a simulation pilot rating of 2 to the overall simulation. He added that he would rate both the GPAS and XB-70 5.5 on the handling-qualities scale.

The responses to an aileron step in the original and the final GPAS configurations are compared in figure 29.

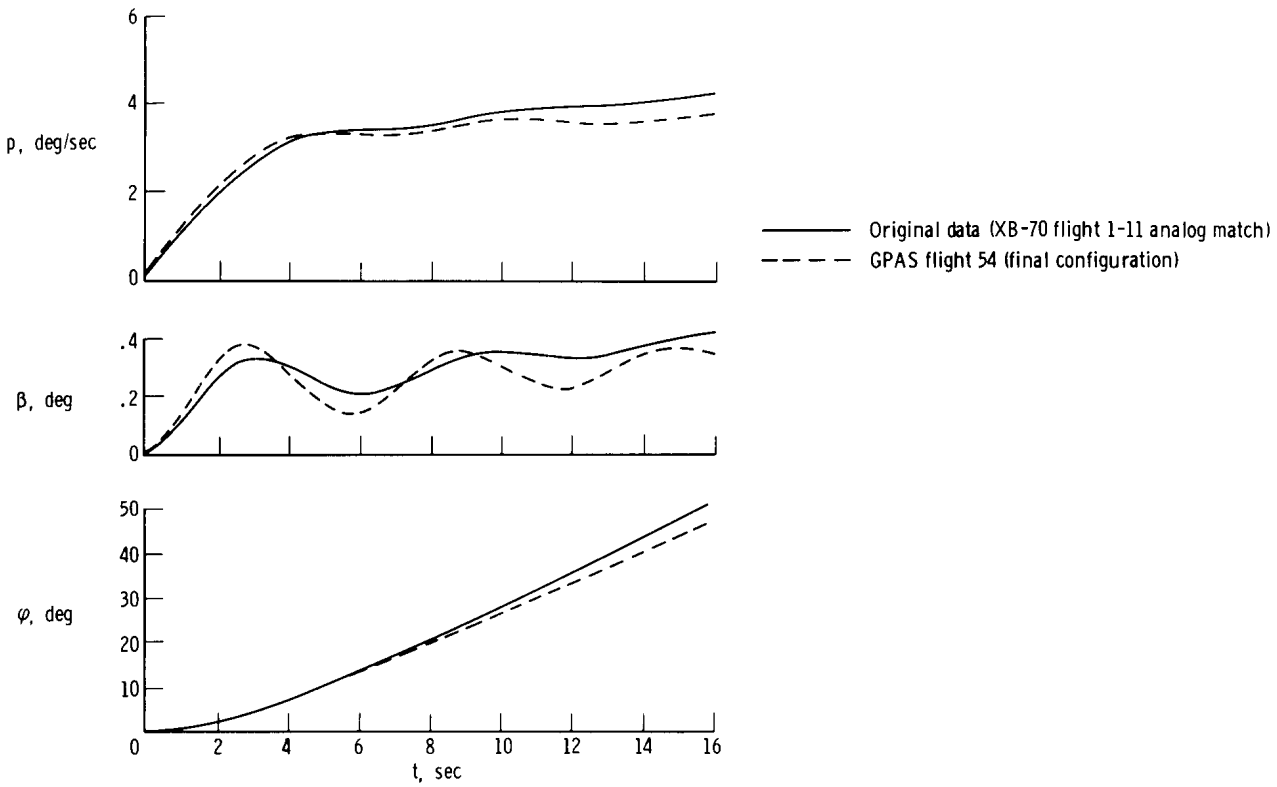

Figure 29. Response of airborne computer to 1° aileron step at $t = 0$ sec. Mach 2.35 simulation.

Simulation of Longitudinal Characteristics

As in the Mach 1.2 validation flights, minimum effort was put into the validation of the longitudinal mode. Only short-period dynamics were examined, because they evolved from flight-obtained derivatives.

The pilot performed several pullups and releases in the GPAS and attempted to perform them in the same manner as they had been in the XB-70. His comments are presented in appendix G. The short-period dynamics are compared in the next section. The pilot thought the GPAS simulation was good and rated the simulation 2. No attempt was made to correct the discrepancy noted in force required in the pullup.

ANALYSIS OF XB-70 FLIGHT 1-68 AND COMPARISON WITH RESULTS OF GPAS FLIGHT 54

This section examines the final configuration reached on GPAS flight 54 and compares it with the second analog-match results and measured XB-70 characteristics. The flight data used to initially program the computer on GPAS flight 54 were obtained from analog-matching a pullup and release and a release from sideslip in XB-70 flight 1-11. The aerodynamic data and associated dynamic characteristics are presented in table 12.

TABLE 12.–AERODYNAMIC DATA AND DYNAMIC CHARACTERISTICS FOR THE XB-70 AT MACH 2.35 FROM ANALOG MATCH OF FLIGHT 1-11

Lateral-directional:			
Geometric characteristics -			
Distance from center of gravity to pilot's station, m (ft)			32 (105)
Gross weight, kg (lb)			177,000 (390,000)
Center of gravity, percent mean aerodynamic chord			21.9
Angle of attack, deg			4.4
True airspeed, m/sec (ft/sec)			698 (2290)
Dynamic pressure, N/m^2 (lb/ft^2)			34,600 (723)
I_{XX}, kg-m^2 (slug-ft^2)			2.546×10^6 (1.878×10^6)
I_{ZZ}, kg-m^2 (slug-ft^2)			30.32×10^6 (22.36×10^6)
I_{XZ}, kg-m^2 (slug-ft^2)			-1.194×10^6 (-0.881×10^6)
Nondimensional derivatives (flight data), per rad -			
$C_{Y_{\delta_a}}$	0.00745	$C_{l_{\delta_a}}$ 0.00442	$C_{n_{\delta_a}}$ -0.00197
$C_{Y_{\delta_r}}$	0.09535	$C_{l_{\delta_r}}$ 0.00069	$C_{n_{\delta_r}}$ -0.02991
C_{Y_r}	0	C_{l_r} -0.02455	C_{n_r} -0.49900
C_{Y_β}	-0.34609	C_{l_β} 0.01068	C_{n_β} 0.05827
C_{Y_p}	0	C_{l_p} -0.08207	C_{n_p} -0.07300
Dynamic characteristics -			
ω_ψ, rad/sec			1.005
ζ_ψ			0.163
τ_r, sec			2.18
τ_s, sec			-61.8
$\left\lvert\frac{\varphi}{\beta}(s)\right\rvert_\psi$			2.16
Angle $\frac{\varphi}{\beta}(s)_\psi$, deg			-171.8
$\frac{\omega_\varphi}{\omega_\psi}$			1.16
p_{ss}, deg/sec/deg			3.28
Longitudinal:			
Geometric characteristics -			
Gross weight, kg (lb)			187,200 (412,700)
Center of gravity, percent mean aerodynamic chord			20.8
Angle of attack, deg			4.4
True airspeed, m/sec (ft/sec)			687.3 (2255)
Dynamic pressure, N/m^2 (lb/ft^2)			36,100 (755)
I_{YY}, kg-m^2 (slug-ft^2)			29.3×10^6 (21.6×10^6)
Nondimensional stability derivatives (flight data, except those with asterisks), per rad -			
$*C_{D_V}$	+0.0000004	C_{L_α} 1.524	C_{m_α} -0.1290
$*C_{D_\alpha}$	-0.1295	$C_{L_{\delta_e}}$ 0.0391	$C_{m_{\delta_e}}$ -0.0412
$*C_{T_V}$	0		C_{m_q} -0.796
Dynamic characteristics -			
ω_{sp}, rad/sec			1.51
ζ_{sp}			0.16
ω_p, rad/sec			0.0169
T_p, sec			371
ζ_p			-0.07
n_{z_α}, g/deg			17.1

Longitudinal

As for the Mach 1.2 validation flight, the pilot evaluated the longitudinal simulation for a pullup and release, considering only the short-period dynamics. Figure 30 shows data from a pullup and release performed on XB-70 flight 1-68 and the analog-computer response during a pullup on the GPAS. The computer response agrees well

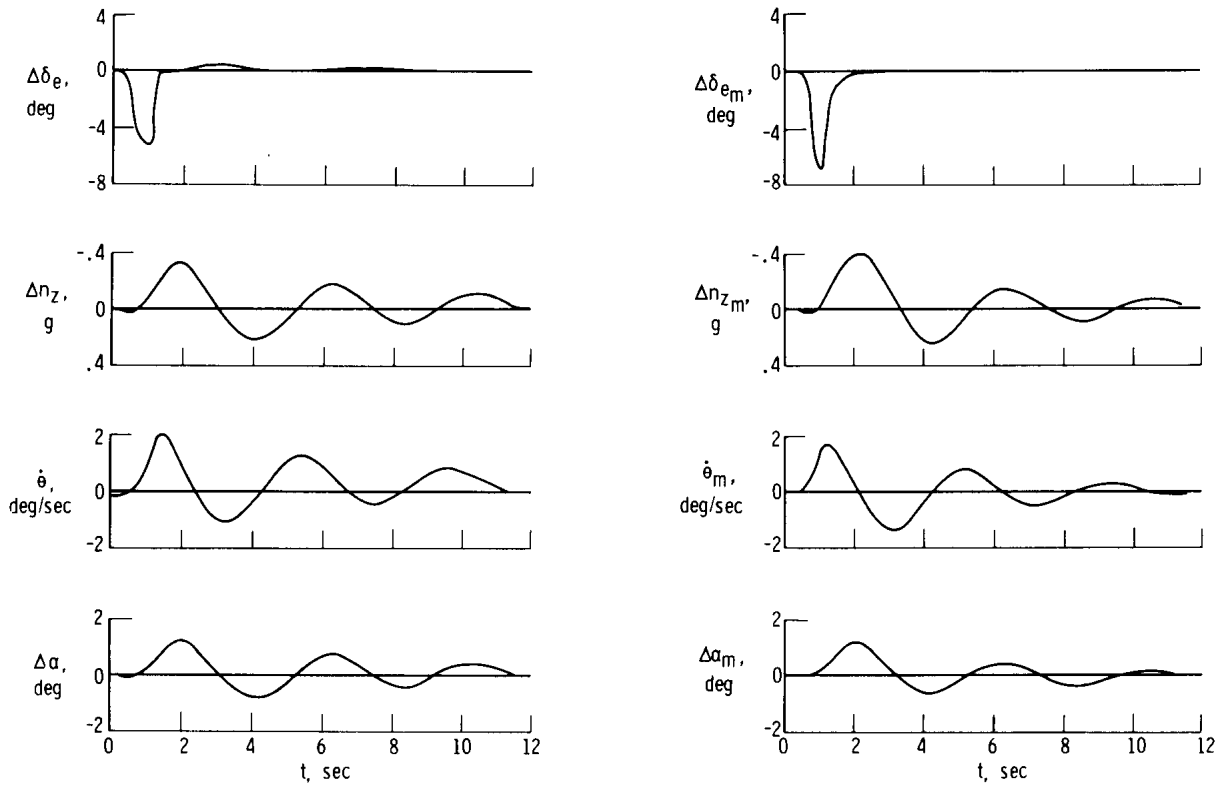

(a) XB-70 flight 1-68. *(b) GPAS flight 54 (analog computer).*

Figure 30. Comparison of XB-70 and GPAS pullup and release maneuver. Mach 2.35 simulation.

with the XB-70 response. The GPAS response is shown in figure 31. Model-following is good, and the GPAS acceleration levels are close to those computed for the model. The angle-of-attack match is good, with the pitch rate of the JetStar behind the model by 0.3 second. The close match of normal-acceleration levels is coincidental, as shown in the following expressions by the n_{z_α} of the model and JetStar in the short-period mode:

Model (XB-70, Mach 2.35) -

$$n_{z_\alpha} \cong \frac{V_T}{g} L_\alpha = \frac{2250}{32.2}(0.244) = 17.0$$

JetStar (Mach 0.55) -

$$n_{z_\alpha} \cong \frac{V_T}{g} L_\alpha = \frac{570}{32.2}(1.1) = 19.6 \text{ (17.8 measured)}$$

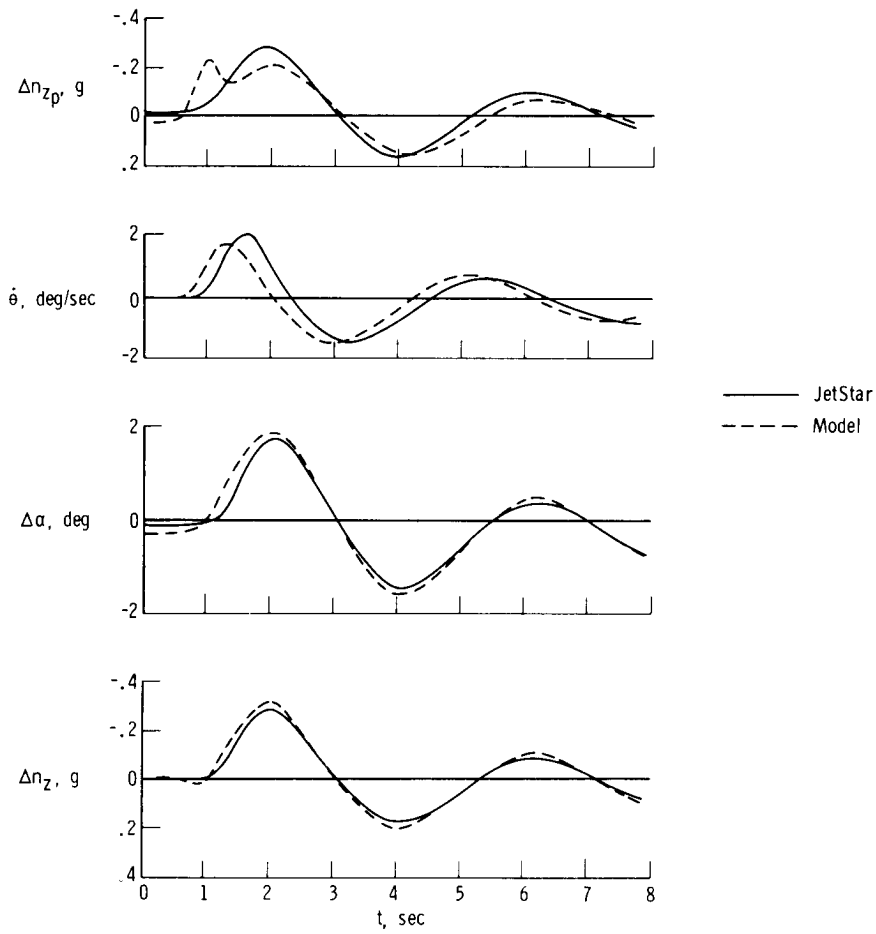

Figure 31. Pullup and release maneuver on GPAS flight 54. Mach 2.35 simulation.

If angle of attack is matched on a 1:1 basis, it is apparent that the resulting match of n_z in a short-period oscillation (hands off) is due to coincidental values of $V_T L_\alpha$ of the XB-70 and the JetStar.

Table 13 compares the longitudinal characteristics programed on the airborne computer with measured XB-70 and JetStar responses. The short-period frequencies agree well. The measured GPAS short-period damping ratio (0.17) agrees well with that programed on the computer but is higher than the measured XB-70 damping ratio. This is attributed to slight elevator float in the XB-70, which was observed to be 180 out of phase with $\dot{\alpha}$. This equivalent $C_{m_{\dot{\alpha}}}$ augmentation reduces the aircraft damping ratio. This floating-elevator effect was not included in the model equations of motion, hence the damping discrepancy.

The model phugoid characteristics were reproduced on the pilot's instrument panel, as shown in table 13. Because no phugoid parameters, such as ΔV, $\dot{h}$, or $\Delta\theta$, were matched, there was no corresponding JetStar motion related to the model phugoid mode.

The discrepancy in $\frac{F_e}{n_z}$ is caused by steady-state errors in angle-of-attack following and a mismatch of the steady-state n_{z_α} response resulting from these errors.

TABLE 13. – COMPARISON OF LONGITUDINAL CHARACTERISTICS OF XB-70 AND GPAS FOR THE MACH 2.35 SIMULATION

Parameter	Measured on XB-70 (flight 1-68)	Programed on GPAS (computer)	Measured on GPAS (flight 54)
ω_{sp}, rad/sec	1.47	1.51	1.53
ζ_{sp}	.11	.16	.17
T_P, sec	Not measured	371	354*
ζ_P	Not measured	-.07	0*
n_{z_α}, g/rad	17.0	17.4	17.8
$\frac{F_e}{n_z}$, N/g (lb/g)	220 (49)	250 (55)	360 (80)

*Airborne computer response measured.

Lateral-Directional

Time histories of rudder and aileron doublets from XB-70 flight 1-68 were analyzed and analog-matched after the GPAS validation flight. The resulting stability derivatives and modes were then compared with the final configuration reached on GPAS flight 54 primarily to determine why changes were necessary in the original aerodynamic data programed on the airborne computer to satisfy the pilot.

Time histories from GPAS flight 54 showed that model-following was generally good, as illustrated in figure 32. Comparisons of model-following fidelity for the two XB-70 flight conditions simulated revealed that the lag in roll-rate (and bank-angle) following was consistently larger for the simulated Mach 2.35 condition than for the Mach 1.2 condition. The roll-rate lags were occasionally as large as 0.5 second, but typically from 0.35 second to 0.4 second. Typical measured values of lag during the Mach 1.2 simulation varied from 0.15 second to 0.25 second. As discussed in the Mach 1.2 analysis section, the lags in roll-following for that condition resulted in a close match of total XB-70 lags; hence, the 0.35 second to 0.40 second of lag in roll-following measured on flight 54 contains 0.1 second to 0.15 second of excess lag, that is, lag greater than would be encountered by the pilot in the XB-70. The effects of this excess lag on the total presentation to the pilot would not be expected to be gross but possibly significant in a condition characterized by a moderate PIO tendency. This factor is considered in the discussion of PIO simulation.

Comparison of Stability Derivatives and Dynamic Characteristics

Two maneuvers from XB-70 flight 1-68 were analog-matched to obtain aerodynamic

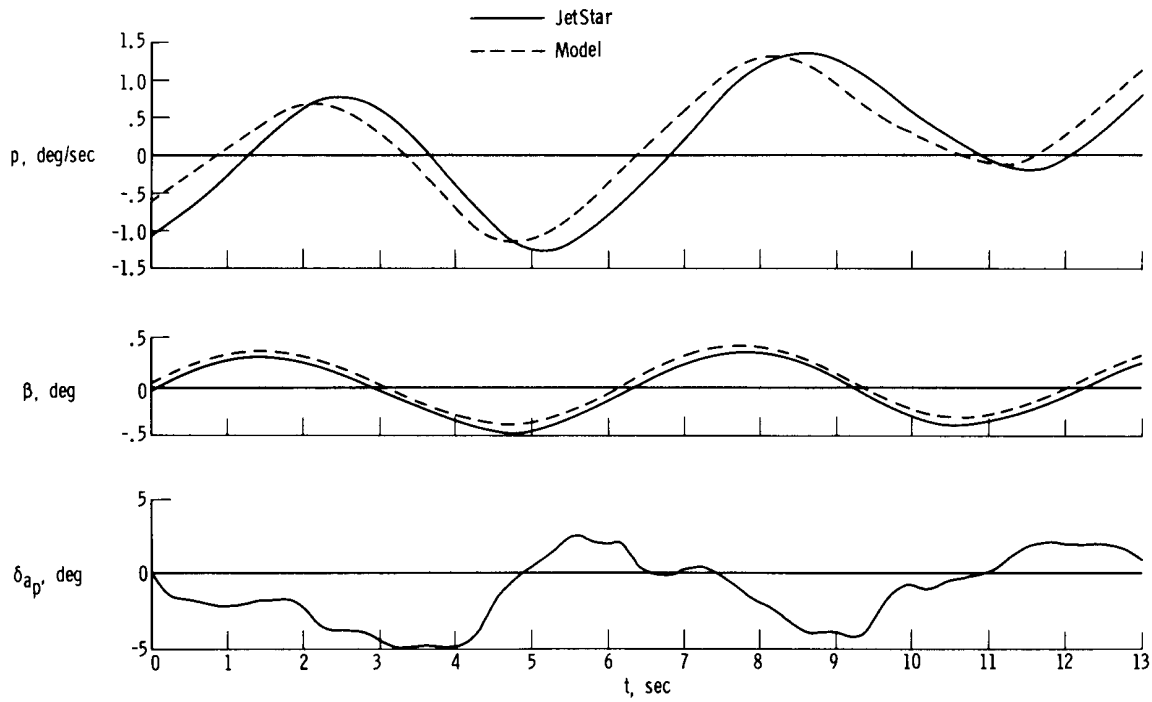

Figure 32. Example of lateral-directional model-following on GPAS flight 54.

stability derivatives for the Mach 2.35 condition. The stability derivatives obtained from this analog match and the original values obtained from analog matches of XB-70 flight 1-11 are presented in table 14. Also included are the derivatives for the final GPAS configuration reached on flight 54.

TABLE 14. – COMPARISON OF STABILITY DERIVATIVES OBTAINED FROM XB-70 ANALOG MATCHING AND GPAS VALIDATION FLIGHT 54

Derivative, rad^{-1}	Original (flight 1-11) data for XB-70	Final GPAS configuration (flight 54)	Best analog match of XB-70 flight 1-68
$C_{Y_{\delta_a}}$	0.00745	0.00745	0.00745
$C_{Y_{\delta_r}}$	.09535	.09535	.09569
C_{Y_β}	-.34609	-.34609	-.3539
$C_{l_{\delta_a}}$	.00442	.00442	.00525
$C_{l_{\delta_r}}$	.000693	.000693	.00304
C_{l_r}	-.02455	-.02455	.000009
C_{l_β}	.01068	.00801	.0091
C_{l_p}	-.08207	-.08207	-.1060
$C_{n_{\delta_a}}$	-.001971	-.00296	-.00072
$C_{n_{\delta_r}}$	-.02991	-.02991	-.02527
C_{n_r}	-.4990	-.2844	-.3280
C_{n_β}	.05827	.05827	.05497
C_{n_p}	-.0730	-.0730	-.1235

The reduction of C_{l_β} and C_{n_r} on the GPAS appears to be justified by corresponding reductions resulting from the analog matches from flight 1-68. The 50-percent increase in $C_{n_{\delta_a}}$ required on the GPAS is not consistent with the value obtained from the flight 1-68 match, which is actually smaller (absolute value) than the original (flight 1-11) value. The increase in $C_{l_{\delta_a}}$ of nearly 20 percent obtained from the flight 1-68 analog match is also significant.

Mode comparison. – Several significant parameters calculated for the three configurations of table 14 are shown in table 15. The final GPAS configuration and the best analog-match data agree favorably in terms of ω_ψ, τ_r, $\left|\frac{\varphi}{\beta}(s)\right|_\psi$, $\frac{\omega_\varphi}{\omega_\psi}$, and p_{ss}. It appears that the reduction of $\left|\frac{\varphi}{\beta}(s)\right|_\psi$ required by the pilot on the GPAS was justified. The pilot's sensitivity to this parameter at this condition is surprising. The spiral mode of the final GPAS configuration is essentially neutral. The flight 1-68 analog match results in a calculated τ_s value of -96 seconds. This value actually differs little from the τ_s value of -245 seconds for the final GPAS configuration in terms of detection by the pilot; both time constants are characteristic of a very weak spiral mode.

TABLE 15. – COMPARISON OF DYNAMICS OF FOUR CONDITIONS RELATING TO MACH 2.35 VALIDATION

Parameter	Flight 1-11 match	GPAS flight 54 final result	Flight 1-68 match	Measured XB-70 flight 1-68
ω_ψ, rad/sec	1.00	1.04	1.00	1.00
ζ_ψ	.163	.094	.133	.13
τ_r, sec	2.17	2.0	2.05	----
τ_s, sec	-61.8	-244.7*	-95.7	----
$\left|\frac{\varphi}{\beta}(s)\right|_\psi$	2.16	1.37	1.58	1.45
Angle $\frac{\varphi}{\beta}(s)_\psi$, deg	-172	-163	-169	-180
$\frac{\omega_\varphi}{\omega_\psi}$	1.16	1.12*	1.10	----
p_{ss}, deg/sec/deg	3.27	2.97	2.89	----

*Calculated.

Frequent pilot comments on the rolloff tendency of the XB-70 at Mach 2.35, however, indicate that both time constants mentioned are most likely too large. Pilot B stated that the original configuration, with τ_s = -62 seconds, displayed only hints of the rolloff characteristic; thus, it must be assumed that the XB-70 has a more strongly divergent spiral than that presented to the pilot on the GPAS. A comment made after the XB-70 flight suggested that this rolloff tendency required frequent pilot inputs which

aggravated the PIO by putting the pilot in the loop.

Probably the most significant difference between the GPAS result and the "best" XB-70 values is in Dutch roll damping. The damping level required in the GPAS ($\zeta_\psi = 0.094$) is somewhat less than measured values for the XB-70 ($\zeta_\psi = 0.13$). The pilot initially required a reduction in the GPAS Dutch roll damping from $\zeta_\psi = 0.16$ to near $\zeta_\psi = 0.10$ to more closely match the XB-70 time to damp. Further adjustments in ζ_ψ were made to adjust the PIO characteristics to more accurately reflect what the pilots saw in the XB-70. Because of the sensitivity of the PIO condition to Dutch roll damping, conclusions regarding the cause of the damping discrepancy are presented at the end of the discussion of PIO simulation.

PIO characteristics of the GPAS and XB-70. – The oscillations induced by the pilot during a wings-level sideslip maneuver on the XB-70 and the GPAS (final configuration, flight 54) are compared in figures 33(a) and 33(b). The aileron workload, which pilot B considered to be important to simulate, is similar for both vehicles. The generation of sideslip during wheel manipulation is also similar for the two vehicles. Bank-angle disturbances during the forced oscillation appear to be less severe for the GPAS, although the pilot stated that these rolling motions matched fairly closely what he experienced in the XB-70. Actual XB-70 time histories show a larger amount of roll oscillation; thus, it is likely that the pilot's impressions of such motion are different in the two vehicles, either because of instrument (attitude display) sensitivity or response or out-the-window field of view. In general, however, the PIO characteristics are similar.

In contrast, the same maneuver is shown in figure 33(c) for the original GPAS configuration, which used stability derivatives obtained from XB-70 flight 1-11. The aileron control motions are obviously more pronounced, as the pilot noted (table 11). The sideslip generation and bank-angle motions are similar to those of the XB-70 (fig. 33(a)). The pilot commented that the GPAS appeared to have too much "rolling" in this manuever.

The frequency of oscillation of both the original and the final GPAS configurations was slightly higher than that of the XB-70 because the XB-70 had a floating rudder effect with sideslip which was not included in the XB-70 model. The overall effect of this discrepancy is minor.

The pilot was questioned about apparent lag in GPAS roll response following pilot control application. He commented that he could detect no difference between the XB-70 and GPAS. Additional lags in the GPAS control system would be expected to make the PIO condition either worse than that in the XB-70, if the XB-70 modeling was reasonably good, or the pilot expend more effort to attain the same performance in the GPAS as in the XB-70. Table 15 indicates that the GPAS modeling of the XB-70 had to be made slightly worse (with respect to ζ_ψ) than in the XB-70 to yield similar PIO characteristics. Thus, the measured excess lags in the GPAS are not in the proper direction to explain the noted differences between the required GPAS configuration and the XB-70. It is not known whether reduction of the GPAS lags to more closely simulate the XB-70 control system would have required further worsening of the XB-70 model to duplicate the XB-70 PIO situation.

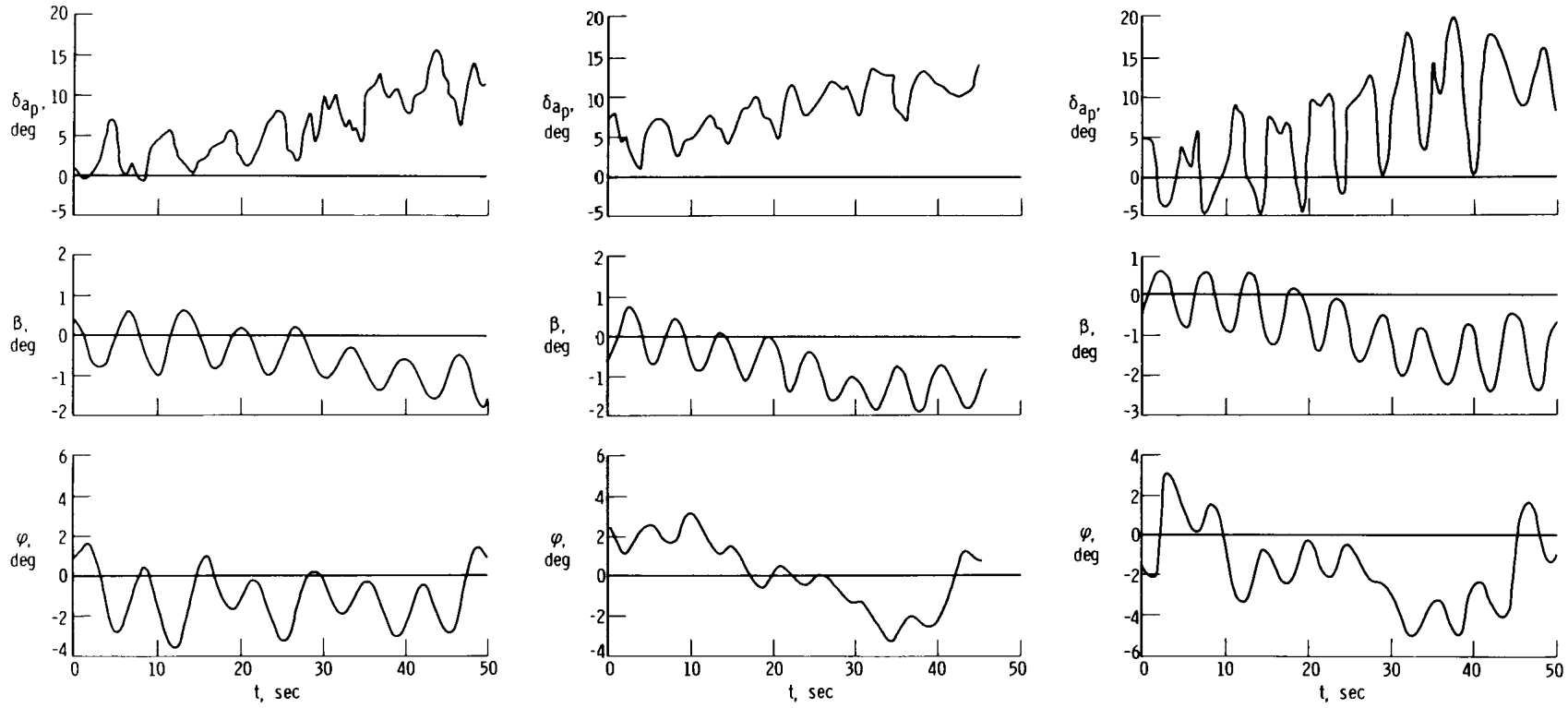

(a) XB-70 Mach 2.35 (flight 1-68).

(b) GPAS final configuration (flight 54).

(c) GPAS original configuration (flight 54).

Figure 33. Comparison of XB-70 and GPAS PIO.

The lateral acceleration at the pilot's location is also significant with respect to the PIO condition. Figure 34 is a comparison of n_{y_p} for the XB-70 during flight 1-68 and for the original and final GPAS configurations of flight 54. The GPAS time histories are those of the JetStar, not the computer. The n_{y_p} responses are similar in magnitude; however, a precise measurement of the phasing between δ_{a_p} and n_{y_p} is difficult because of the highly active nature of the pilot's control application. As discussed in more detail in reference 5, this similarity in acceleration levels at the cockpit is not the result of an attempt to match this parameter in the GPAS, but rather the result of several fortunate coincidental geometric and aerodynamic characteristics of the XB-70 and JetStar. In addition, the pilot commented that he felt approximately the same very small amount of side force in the JetStar as he had in the XB-70.

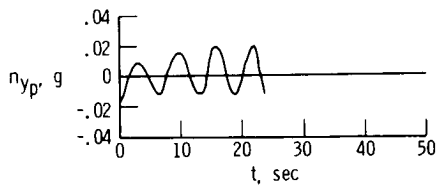

(a) XB-70 flight 1-68.

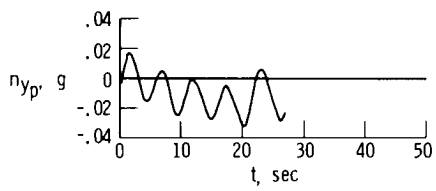

(b) Original GPAS flight 54 configuration (actual JetStar motion).

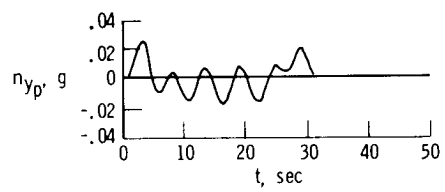

(c) Final GPAS flight 54 configuration (actual JetStar motion).

Figure 34. Lateral acceleration at the pilot's location during a PIO in the XB-70 and GPAS. (Pilot inputs not necessarily the same for all three conditions.)

It appears that the pilot directed the GPAS to be changed from the original configuration to one which more accurately duplicated his activity during a PIO. He required ζ_ψ to be slightly lower than measured for the XB-70 and $C_{n_{\delta_a}}$ to be higher than the value obtained from analog-matching. No single obvious reason can be found to satisfactorily explain these two discrepancies, but the following factors may have contributed:

(1) The lack of a moderately divergent spiral mode on the GPAS may have lessened the requirements for pilot correction, making the GPAS appear better from the standpoint of PIO initiation. The pilot's requests for a general worsening of the original GPAS configuration then could have been, in part, an attempt to compensate for the absence of the destabilizing influence of the rolloff tendency which was apparently prevalent in the XB-70.

(2) The analog-match results from flight 1-68 show a $C_{l_{\delta_a}}$ nearly 20 percent higher than that obtained originally. This higher value may indicate that a proportionately lower pilot gain would be required to drive the Dutch roll into a neutral or unstable condition. This example is indicative of the fact that the XB-70 may have the same PIO characteristics as obtained on the GPAS, but for slightly different reasons.

(3) The ability of the pilot to exactly duplicate a condition he flew previously may have a large enough uncertainty associated with it to be a factor.

Although the discrepancy in ζ_ψ and $C_{n_{\delta_a}}$ should not be ignored, the fact that all three conditions the pilot saw did not differ grossly warrants an endorsement of the GPAS capabilities in representing this XB-70 condition. Even the original GPAS configuration was given a simulation pilot rating of 3+, with the additional pilot comment that it was not unrepresentative.

Time-history comparison. – An aileron doublet followed by mild aileron maneuvering in flight 1-68 of the XB-70 was recorded on an FM tape recorder for playback directly into the GPAS in flight. Figure 35 shows the XB-70 and GPAS responses. The GPAS response is that of the JetStar itself for the final configuration of flight 54. (The second analog-matched data were not available at this time.) The JetStar response compares favorably with the actual XB-70 response. The JetStar yaw rate and sideslip are of larger magnitude than those of the XB-70, but the lateral accelerations at the cockpit for the two vehicles are similar, a fortunate situation because sideslip and bank angle were the only parameters directly matched in the GPAS. The overall fidelity of the lateral-directional simulation was termed "very good" by pilot B.

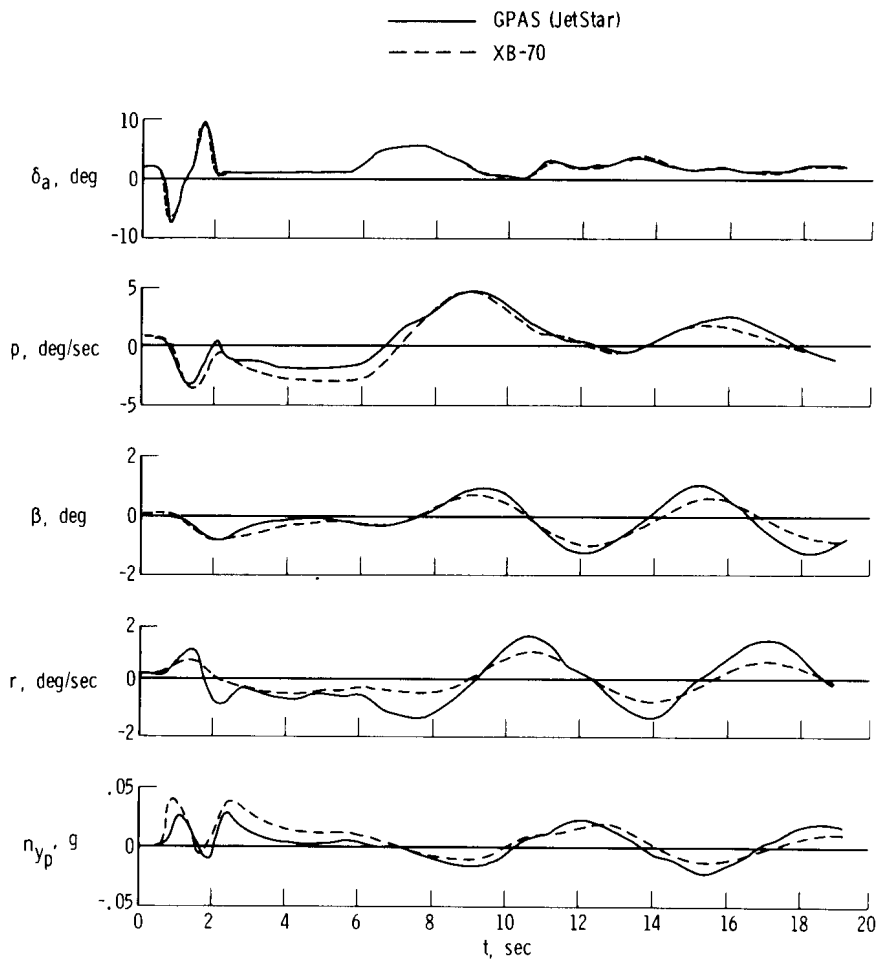

Figure 35. Comparison of XB-70 and GPAS responses to double aileron pulse. GPAS flight 54; final configuration; Mach 2.35 simulation.

Additional Analysis of Feel-System Discrepancies

From the information available, it was determined that the XB-70 aileron feel system had the following static characteristics:

Force gradient	3.1 N/deg (0.70 lb/deg) wheel
Breakout force	8.9 N (2.0 lb)
Double hysteresis	18 to 22 N (4.0 to 5.0 lb)

The GPAS feel system was set up originally to duplicate all three of these characteristics. However, even at moderate wheel-deflection rates, it was observed that the GPAS hysteresis increased noticeably over that programed because of what may be termed "dynamic hysteresis," which is hysteresis due to the time delay between force command and position response. This hysteresis would be in addition to any amount added artificially. To avoid presenting the pilot an excess of apparent hysteresis, no artificial hysteresis was added to the basic aileron feel setup. This still resulted in excess hysteresis, however, for moderate rate inputs.

The XB-70 pilots who evaluated the GPAS feel system commented that the aileron forces appeared to be higher than those of the XB-70. It was also difficult for them to describe exactly what was incorrect about the setup of the GPAS feel system. During early XB-70 simulation flights, pilot A believed that the problem was in the gradient and finally settled on a value of 2.2 N/deg (0.50 lb/deg), which was slightly lower than the measured XB-70 value of 3.1 N/deg (0.70 lb/deg). During the Mach 2.35 simulation validation flight, pilot B thought the problem was in the breakout force representation and requested that it be removed. When this was done, he believed the GPAS feel system was close enough to that of the XB-70 for his evaluation purposes.

Careful examination of XB-70 aileron feel control cycles failed to show either change to be justified. The XB-70 static characteristics were as had been originally programed. Because the net effect of a low bandwidth feel system is an apparent increase in force required for increased wheel rates, it is probable that each pilot compensated for this by requesting that the static characteristics be altered.

Similar experiences were encountered with the rudder and elevator feel systems. Most of the complaints were made about the rudder feel system, especially for sharp rudder kicks in which the rudder forces seemed to be high and the movement sluggish. To make the rudder feel more representative of the XB-70, pilot A requested that the breakout force and gradient be reduced. Pilot B had similar comments, but did not request a change.

Pilot opinion of feel characteristics with and without the associated dynamics of the simulated characteristics is also of interest. Pilot A stated that the GPAS aileron feel system felt artificial on the ground but realistic in the air. Pilots A and B both thought the GPAS feel system was easier to evaluate while they were flying the vehicle simulation. They stated further that evaluating the feel system simulation was, in some respects, more difficult than judging the fidelity of the vehicle dynamics. In some instances, they were able to pinpoint actual errors in the feel setup, but more often they were unable to isolate the problem area although they knew something was wrong.

Feel system discrepancies elicited more pilot comment than any other single item in the GPAS simulation. Although the quantitative effects of such discrepancies on the apparent aircraft handling qualities are unknown, the nuisance factor was enough to annoy the pilot. The distracting influence of such discrepancies cannot be overlooked and probably is reason enough to place high priority on feel-system setup in future handling-qualities studies.

Conclusions on the Validation With the XB-70 at Mach 2.35

The GPAS duplicated the lateral-directional dynamics and the longitudinal short-period dynamics of the XB-70 at Mach 2.35 and 16,800 meters (55,000 feet) altitude, according to the XB-70 evaluation pilot. The pilot was able to detect some discrepancies in the original configuration and requested changes in the airborne computer to bring the GPAS closer to the actual XB-70 dynamics. The pilot assigned an SPR of 2.0 to the GPAS and rated both the XB-70 and GPAS 5.5 on the handling-qualities scale.

The resultant GPAS configuration agreed favorably, in most respects, with measured and recorded XB-70 characteristics. The GPAS Dutch roll damping ratio was slightly lower than measured XB-70 values, and, until this discrepancy is satisfactorily explained, it must be assumed that the GPAS may introduce errors in apparent damping ratio of at least $\Delta\zeta_\psi = 0.04$ (0.133 to 0.94) in the region of $\zeta_\psi = 0.1$. Future experiments with incremental changes in ζ_ψ less than this value may not be valid.

Lateral acceleration at the GPAS pilot's location closely matched that of the XB-70 at this condition, but only because of a fortunate set of circumstances which, in most instances, would not occur.

CONCLUDING REMARKS

A flight simulation program was conducted to validate the general purpose airborne simulator (GPAS) for handling-qualities studies of large transport airplanes in cruise. According to the ground rules of the program, the XB-70-1 airplane was to be simulated accurately and realistically. Time histories showed that the GPAS was capable of high-quality reproduction of model dynamic characteristics. Also, when the model was a good representation of the XB-70, the pilots commented favorably on the simulation. These results indicated that the GPAS was capable of simulating the type of cruise dynamics typical of a large supersonic aircraft.

The most difficult and time-consuming task in the validation program was defining an accurate model of the XB-70. Several analog matches and in-flight changes were necessary before a satisfactory simulation was obtained. Of course, this problem is not peculiar to airborne simulators. It should be recognized that what determines the effectiveness of a reasonably well-configured simulator is likely to be the quality of data used to program it. Nothing in the validation program suggested that the in-flight environment made model discrepancies any more acceptable; if anything, the opposite was true.

It is important to note that the simulation fidelity was apparently degraded when pilots took liberties with the simulator that they would not take with the actual vehicle. These instances were rare in the GPAS, however, which suggests that one primary value of the actual in-flight environment provided by the airborne simulator is to aid the pilot in creating the illusion that he is in the actual vehicle. Since such an illusion influences pilot response, it may be important in a particular simulation.

Simulation compromises in motion and visual cues were seemingly justified on the basis of the reasonably good resulting simulations. In a cruise configuration, however, cue conflicts are less likely to pose problems than in a landing simulation, for example. Turn-rate mismatch for a given bank angle was noticed by the pilots but was not objectionable. It is doubtful whether this would be true in the approach. Similarly, flight-path changes (speed and altitude) which are nearly visually imperceptible at altitude become primary cues near the ground. Thus, the compromises which must be made for a simulation are varied, depending on the task.

Several techniques used in the GPAS validation program appear to be applicable to other cruise simulations. These include:

(1) The use of a simulation pilot-rating scale to rate the simulator against the actual aircraft or to rate a fixed-base simulator against a motion simulator.

(2) The use of uncoupled model equations for conservatively flown cruise-flight conditions.

(3) The exclusive use of computer-driven flight instruments for cruise-condition simulation.

(4) The use of taped inputs to enable comparisons to be made between GPAS response and actual vehicle or other simulator response.

Flight Research Center,
National Aeronautics and Space Administration,
Edwards, Calif., December 10, 1970.

APPENDIX A

EQUATIONS OF MOTION PROGRAMED ON AN AIRBORNE ANALOG COMPUTER

Two independent sets of three-degree-of-freedom equations of motion were used for the longitudinal and lateral-directional representations of the XB-70 on the airborne analog computer. The equations were in a linearized, perturbation form. The angular positions, rates, and accelerations are in degrees, degrees/second, and degrees/second^2, respectively.

LONGITUDINAL (X-WIND AXIS, Y- AND Z-BODY AXES)

X-force

$$\Delta\dot{V} + D_V\Delta V + \frac{V_T D_\alpha}{57.3}\Delta\alpha + \frac{g}{57.3}\Delta\theta = \frac{\Delta T}{M}$$

Z-force

$$\frac{\alpha_T}{V_T}\Delta\dot{V} + \Delta\dot{\alpha} - Z_\alpha\Delta\alpha - \Delta\dot{\theta} - Z_\theta\Delta\theta = Z_{\delta_e}\Delta\delta_e$$

Pitching moment

$$-M_{\dot{\alpha}}\Delta\dot{\alpha} - M_\alpha\Delta\alpha + \Delta\ddot{\theta} - M_q\Delta\dot{\theta} = M_{\delta_e}\Delta\delta_e + (57.3)M_{\Delta T}\Delta T$$

LATERAL-DIRECTIONAL (BODY AXES)

Y-force

$$-\frac{\alpha_T}{57.3}\dot{\varphi} - \frac{g}{V_T}\varphi + \left[1 + \left(\frac{\alpha_T}{57.3}\right)^2\right]r + \dot{\beta} - Y_\beta\beta = Y_{\delta_r}\delta_r$$

Rolling moment

$$\ddot{\varphi} - L_p\dot{\varphi} - \left(\frac{I_{XZ}}{I_{XX}} + \frac{\alpha_T}{57.3}\right)\dot{r} + \left(\frac{\alpha_T}{57.3}L_p - L_r\right)r - L_\beta\beta = L_{\delta_r}\delta_r + L_{\delta_a}\delta_a$$

Yawing moment

$$-\frac{I_{XZ}}{I_{ZZ}}\ddot{\varphi} - N_p\dot{\varphi} + \left[1 + \left(\frac{\alpha_T}{57.3}\right)\frac{I_{XZ}}{I_{ZZ}}\right]\dot{r} + \left(\frac{\alpha_T}{57.3}N_p - N_r\right)r - N_\beta\beta = N_{\delta_r}\delta_r + N_{\delta_a}\delta_a$$

APPENDIX B

SUMMARY OF PILOT COMMENTS ON XB-70 FLIGHT 1-63

The nose ramp was up for the $M = 1.2$ tests at 40,000 feet.

At $M = 1.4$ and 32,000 feet there was no tendency to roll out of a bank. There was nothing strong there. The spiral is very weak. The point may not be good for quantitative information, but qualitatively it tells me that if the GPAS spiral is strong, it's wrong.

Double aileron and double rudder pulses produced maximum sideslip excursions of 2°.

The yaw needle was dead in 3 1/2 cycles.

In the wings-level sideslip I got to full rudder; got 3.2° of sideslip holding 2° to 3° of wheel. There was no evidence of a shelf in C_{n_β} at this condition.

The XB-70 control wheel does not have good centering.

I can't say that anytime today I felt side force.

Roll power was more than I needed, but it was not objectionable.

I have never been worried about turbulence from a handling standpoint. The XB-70 flight path is not disturbed much by turbulence.

Adverse yaw due to aileron is light--less than in other conditions on the XB-70. I'll rate it 2 on the basis of Dutch roll damping and adverse yaw.

The longitudinal damping was excellent.

The ability to do a wings-level sideslip I will rate 1, and the ability to make precise heading changes, 2.

I get 3/4° of sideslip in a slow roll and 1 1/2° in a fast roll.

APPENDIX C

FLIGHT PLAN FOR VALIDATION PORTION OF GPAS FLIGHT 45

GENERAL INSTRUCTIONS

The purpose of this flight is to validate the GPAS by simulating the XB-70 behavior. The XB-70 flight condition is Mach 1.2 at 40,000 feet, tips 25°, and stability augmentation off. The pilot performs maneuvers on the GPAS in order to compare the response with the XB-70. Changes will be made, if possible, to correct or minimize noted discrepancies.

PILOT COMMENT CARD

LONGITUDINAL

Compare the following GPAS characteristics with the XB-70:

1. Feel system (δ_{e_p})
   a. Force gradient
   b. Breakout force
   c. Centering
2. Short-period dynamics
   a. Frequency
   b. Damping
3. Stick force per g
4. Ability to hold g
5. Ability to hold attitude
6. Ability to make small changes in altitude (±1000 ft)
7. Pitch rate evaluation
   a. Initial response from trim
   b. Steady pitch rate after transient response
8. Ability to trim at new airspeed (±0.1 M)
9. Speed response to throttle
10. Overall simulation fidelity
    a. Environment (switches, instruments, cabin noise, visibility)
    b. Motion cues
11. Overall longitudinal pilot rating
12. Any other comments or maneuvers

APPENDIX C

LATERAL-DIRECTIONAL

1. Aileron feel
   a. Force gradient
   b. Breakout force
   c. Centering
   d. Anomalies
2. Rudder feel
   a. Force gradient
   b. Breakout force
   c. Centering
   d. Anomalies
3. Dutch roll dynamics
   a. Frequency
   b. Natural damping
   c. Pilot technique in damping Dutch roll
4. Wings-level sideslip
   a. Indicated yaw angle
   b. Aileron wheel angle
   c. Percent of rudder pedal
5. Roll power
   a. Roll rate
   b. Roll damping
6. Yaw due to aileron
   a. Magnitude for given wheel input
   b. Does yaw angle or roll angle change first?
7. Spiral stability (release from small bank angle)
8. Dihedral effect (roll off with rudder)
9. Response in the lateral-directional maneuver
10. Rudder power or effectiveness
11. Ability to make precise heading changes with aileron only
12. Overall simulation fidelity
    a. Environment (switches, instruments, cabin noise, visibility)
    b. Motion cues
13. Overall lateral-directional pilot rating
14. Any other comments or maneuvers

APPENDIX D

PILOT QUESTIONNAIRE FOR HANDLING-QUALITIES EVALUATION OF XB-70 AND GPAS

This questionnaire is not to be used during any flight directly but, rather, indicates the intended scope of the evaluation. It also indicates the types of questions the pilot may be asked.

LONGITUDINAL

1. Elevator feel system
   a. Force gradient
   b. Breakout force and centering
2. Short-period dynamics
   a. Frequency and damping
   b. Acceleration response to elevator
3. Maneuvering flight
   a. Ability to hold attitude
   b. Lags noted in pitch response

LATERAL-DIRECTIONAL

1. Aileron and rudder feel systems
   a. Force gradient
   b. Breakout force and centering
2. Dutch roll dynamics
   a. Frequency and damping
   b. Roll-to-yaw ratio
   c. Excitation of Dutch roll mode
   d. PIO initiation and technique in damping
3. Rolling maneuvers
   a. What limits your maximum roll rate?
   b. Initial roll response--any lags noted?
   c. Amount of bank angle lead needed to stabilize on a target bank angle
   d. Difference in apparent roll power for coordinated and uncoordinated turns. Is coordination easily accomplished?
   e. Ease in making small bank angle changes at comfortable roll rate
4. Rudder power effectiveness
5. Spiral mode--convergence or divergence obvious to pilot?
6. Amount of side force felt

APPENDIX E

PILOT'S REPORT AND COMMENTS ON XB-70 FLIGHT 1-68

PILOT REPORT

Stability and Control and Handling Qualities at Mach 2.35, 55,000 Feet

A good portion of this test series was flown in continuous light turbulence. The [inlet] shock positions were set at 0.60 shock position ratio prior to beginning the stability tests. When all flight augmentation control systems were initially turned off, the airplane immediately developed a ±1° yaw condition even though full pilot attention was being devoted to preventing a PIO. Apparently the oscillation was being amplified by the pilot's lateral control action because the oscillation increased to ±1.5°, at which time all FACS were reengaged. All FACS were disengaged again, and very close pilot attention prevented the PIO from redeveloping. Even with hands off, the airplane continued to display a residual ±1/4° yaw oscillation. The airplane would also tend to roll off in one direction or the other when released. It was extremely difficult to trim for the doublet tests because of the handling qualities and because the left wing heaviness had increased to where approximately 8° of wheel had to be trimmed in to counteract the wing heaviness. An aileron doublet followed by a rudder doublet was superimposed on top of the ±1/4° oscillation. Both doublets went to approximately 1 1/2° of yaw and had positive damping, although about 4 cycles were required to damp to the ±1/4° oscillation. Recovery from each doublet was required as the airplane rolled to 30° bank. Apparently the spiral stability was weak.

A sideslip was performed using full right rudder and 18° of right wheel (10° more than the trim position). The sideslip angle oscillated between 1.5° and 2.0°, and the moderate negative dihedral effect was reconfirmed. A pullup and release from 1.3g had positive damping and damped to one-half amplitude in 2 cycles.

Handling Qualities for GPAS Validation

The airplane was flown for approximately 20 minutes with all FACS off to allow the pilot to obtain qualitative handling data and to establish firm opinions of the handling qualities at Mach 2.35, 55,000 feet. This was done to allow a validation of the XB-70 handling qualities which had been set on the GPAS.

Numerous lateral-directional characteristics were checked, and a few of the more significant are listed. The airplane appeared to be more stable directionally during a bank, because the directional oscillation could be kept around ±1/4° during a bank, but during wings-level flight the oscillations frequently reached ±1°. With bank angles up to 30°, the desired bank angle could be held within ±1° with a normal pilot workload.

An 8° lateral wheel movement applied at a moderate rate would generate 1° of adverse yaw and a one-fourth sideslip ball movement in the opposite direction. The ailerons had light breakout forces with slightly weak centering. Approximately 10 pounds of aileron force were needed to obtain a 10° wheel movement. The roll response was

excellent, but the rolling inertia was not particularly high because the roll stopped quickly when the ailerons were released. The Dutch roll oscillation appeared to be predominantly directional, with very little rolling associated with the oscillations. Rudder breakout forces appeared to be fairly heavy and were estimated to be slightly over 10 pounds. A half rudder input illustrated the negative dihedral effect and caused a roll of approximately 10 degrees per second in the opposite direction. It was very difficult to accomplish satisfactory coordinated turns. The control input could be coordinated fairly well, but, when the controls were returned to neutral, the yaw would frequently reach 1 1/2°. The lateral-directional handling qualities at these conditions were rated as 5.5.

ADDITIONAL PILOT COMMENTS IN DEBRIEFING SESSION FOLLOWING XB-70 FLIGHT 1-68

The wheel force gradient was very shallow ±5° around center.

For a ±1° sideslip, there appeared to be almost no bank-angle oscillation.

A rapid 10° wheel input would produce 1 1/2° of sideslip, not as much as I expected.

Turbulence did not seem to affect controllability of the aircraft.

PIO pilot rating was 3 1/2.

Roll rate which produces 2° of sideslip is the maximum roll rate I use.

I was really a lot more timid about doing things with the XB-70, from a handling qualities standpoint, than in the GPAS.

APPENDIX F

FLIGHT PLAN FOR GPAS FLIGHT 54

PURPOSE

The purpose of this flight is to validate the GPAS for simulation of the cruise characteristics of large transport aircraft. The emphasis will be on the lateral-directional dynamics.

EVALUATION TASK

The evaluation pilot will be asked to compare the flight characteristics of the XB-70 at Mach 2.35 at 55,000 feet, stability augmentation off, wing tips at 65° with those of the GPAS. The pilot will be asked to point out noted discrepancies and to aid in correcting these items. The pilot is requested to make use of the simulation pilot rating scale as he compares the GPAS with the XB-70.

SPECIAL NOTES

It is important that the evaluation pilot perform maneuvers in the GPAS as he would perform them in the XB-70, observing not only ultimate test limits on sideslip, for example, but also personal limits which the pilot observes. It is desirable that the pilot treat the GPAS as he would the XB-70 itself, in all tasks.

EVALUATION AND COMPARISON

The pilot is to make use of his XB-70 flight notes to compare the configuration presented on the GPAS with the XB-70. Evaluate and compare:

1. Feel system.
2. Pullup and release.
3. Double aileron pulse.
4. Double rudder pulse.
5. Wings-level sideslip.
6. Lateral-directional maneuver.
7. Additional rolling maneuvers discussed earlier:
   a. Medium bank-angle maneuvers (20° to 30°) using faster than usual roll rate.
   b. Small bank-angle maneuvers (5° to 10°) using normal roll rates. Make small changes and hold that attitude.

REFINEMENT OF GPAS CONFIGURATION

After the comparison with the XB-70 has been made, the pilot is to single out what

he considers to be the most significant discrepancy between the GPAS configuration and the XB-70. Appropriate changes will be made to the airborne computer by the test engineers with assistance from the pilot. It is requested that the pilot assign simulation pilot ratings where applicable.

After the most serious discrepancy has been corrected, work will be directed toward the next most significant problem area, and so on, as time permits.

COMPLETE EVALUATION OF FINAL CONFIGURATION OBTAINED

The pilot is to evaluate the condition which results from any and all changes made to the GPAS. Comments and ratings are desired for at least the following items:

1. Longitudinal
   a. Elevator feel system.
   b. Short-period frequency and damping.
   c. Normal acceleration response in a pullup.
2. Lateral-directional
   a. Aileron feel system.
   b. Rudder feel system.
   c. Dutch roll dynamics.
   d. Adverse yaw due to aileron.
   e. PIO tendency.
   f. Side force felt.
   g. Roll power.

APPENDIX G

PILOT B COMMENTS ON LONGITUDINAL SHORT-PERIOD SIMULATION OF XB-70 AT MACH 2.35 (GPAS FLIGHT 54)

I think it takes a little less force here to get the g that you get in the XB-70, and the one thing that's missing (and I know you can't simulate) is the fact that in the XB-70 you pull up and then you get this g transmitted to the cockpit with what I'd describe as kind of a small shock. You don't get anything momentarily, and then all of a sudden you feel it come right to the cockpit; you don't feel this way in the GPAS. That's a structural response rather than a dynamic response.

You have the lag in here about right; seems that maybe you've got the force required to get a certain g a little bit lighter than it should be. It's either the force required or else it is less control travel; I'm not sure which. But your actual response looking at your accelerometer seems to be in the ball park. If you're going to rate it as a simulator, I think I'd rate it a 2 as far as the longitudinal short-period simulation is concerned.

REFERENCES

1. Clark, Daniel C.; and Kroll, John: General Purpose Airborne Simulator - Conceptual Design Report. Cornell Aeronautical Laboratory, Inc. (NASA CR-544), 1966.

2. Rediess, Herman A.; and Deets, Dwain A.: An Advanced Method for Airborne Simulation. J. Aircraft, vol. 1, no. 4, July-Aug. 1964, pp. 185-190.

3. Kroll, John; Arendt, Rudy H.; and Pritchard, Francis E.: Development of a General Purpose Airborne Simulator. Cornell Aeronautical Laboratory, Inc. (NASA CR-641), 1966.

4. Berry, Donald T.; and Deets, Dwain A.: Design, development, and utilization of a general purpose airborne simulator. AGARD Rep. 529, May 1966.

5. Szalai, Kenneth J.: Motion Cue and Simulator Configuration Aspects of the Validation of a General Purpose Airborne Simulator. NASA TN D-6432, 1971.

6. Mechtly, E. A.: The International System of Units - Physical Constants and Conversion Factors. NASA SP-7012, 1969.

7. Wolowicz, Chester, H.; Strutz, Larry W.; Gilyard, Glenn B.; and Matheny, Neil W.: Preliminary Flight Evaluation of the Stability and Control Derivatives and Dynamic Characteristics of the Unaugmented XB-70-1 Airplane Including Comparisons With Predictions. NASA TN D-4578, 1968.

8. Harper, Robert P., Jr.; and Cooper, George E.: A Revised Pilot Rating Scale for the Evaluation of Handling Qualities. AGARD Conference Proceedings 17, Stability and Control - Part 1, Sept. 1966, pp. 227-245.

9. Harper, Robert P., Jr.: In-Flight Simulation of the Lateral-Directional Handling Qualities of Entry Vehicles. WADD Tech. Rep. 61-147, Aeronautical Systems Div., Wright-Patterson Air Force Base, Nov. 1961.

NASA-Langley, 1971 — 11 H-591